Interactive Visual Analysis of Time-dependent Flows: Physics- and Statistics-based Semantics

Armin Pobitzer

Dissertation for the degree of Philosophiae Doctor (PhD)

Supervised by Helwig Hauser
Co-supervised by Øyvind Andreassen

Department of Informatics
University of Bergen
Norway

April 2012

ISBN 978-82-308-2063-6
University of Bergen, Norway
Submitted April 23, 2012 (print version 15. juni, 2012)

Scientific Environment

The research work resulting in this thesis has been carried out in the Visualization group at the Department of Informatics, University of Bergen, in context of the collaborative research project "SemSeg – 4D Space-Time Topology for Semantic Flow Segmentation", founded by the European Commission in the *Future and Emerging Technologies (FET) Programme* within the *Seventh Framework Programme for Research* (grand number 226042).

UNIVERSITY OF BERGEN
Department of Informatics

ICT

Research School in
Information and Communication Technology

Acknowledgments

First of all, I would like to thank my supervisor, Helwig Hauser, for taking me on as a student, his support, and numberless fruitful discussions throughout these three years that led up to this thesis. He introduced me to the world of visualization and research. I am also very grateful to my co-supervisor, Øyvind Andreassen, who introduced me to the fascinating world of fluid mechanics, for many insightful conversations on the topic.

In the course of my ph.d. work I had the chance to collaborate with a number of senior researchers, Raphael Fuchs, Krešimir Matković, Ronald Peikert, Holger Theisel, and Murat Tutkun, from whose experience and knowledge I benefited greatly. Thanks to Johannes Kehrer and Ola Kristoffer Øye for his valuable feedback on my thesis. Thank is also due to the *SimVis GmbH* and its staff, Helmut Doleisch, Wolfgang Freiler, and Philipp Muigg, who provided me with their fine framework and supported me whenever I had questions regarding its use. My gratitude goes also to Wolfang Förg-Rob and Ulrich Oberst, who taught me virtually everything I know about higher mathematics in the course of my masters. They laid the mathematical ground for the here presented research.

I acknowledge the financial support for this ph.d. project of the Future and Emerging Technologies (FET) programme within the Seventh Framework Programme for Research of the European Commission (grant number 226042) for the SemSeg project, which I was a part of for the last three years.

I would also like to thank my present and former colleagues from the Visualization group at the University of Bergen, Paolo Angelelli, Åsmund Birkeland, Andrea Brambilla, Johannes Kehrer, Ove Daae Lampe, Endre Mølster Lidal, Mattia Natali, Július Parulek, Daniel Patel, Veronika Šoltészová, and Çağatay Turkay. They where a big part of creating a fun and welcoming work environment. The fact that I regard them not only my colleagues, but they have also become my friends in the course of the last three years, says it all about this extraordinary group of people. Special thanks goes to Andrea Brambilla, who I shared office with for the second half of my ph.d. project, for countless discussion on both work- and a bit less work-related topics over a nice cup of coffee. Without him my caffeine addiction would never have reached its current heights.

Whenever I needed to unwind from my work, I could count on my good friends,

that I made during the last four years here in Bergen. Thanks for a lot of fun, memorable days and nights, and good conversations goes to Aksel, Astri, Bjørn, Craig, who also proofread my English in this thesis, Erik, and Ida.

My unlimited gratitude goes to my parents, Petra and Andreas, my brother Philipp, and my grandparents, and the rest of my family for their everlasting and unconditional love and support along the long road that led up to this pd.h. thesis and my life as it is today. Without them, none of this would have been possible.

Abstract

With the increasing use of numerical simulations in the fluid mechanics community in recent years flow visualization increasingly gains importance as an advanced analysis tool for the simulation output. Up to now, flow visualization has mainly focused on the extraction and visualization of structures that are defined by their semantic meaning. Examples for such structures are vortices or separation structures between different groups of particles that travel together.

In order to deepen our understanding of structures linked to certain flow phenomena, e.g., how and why they appear, evolve, and finally are destroyed, also linking structures to semantic meaning that is not attributed to them by their very definition, is a highly promising research direction to pursue.

In this thesis we provide several approaches on how to augment structures stemming from classical flow visualization techniques by additional semantic information originating from new methods based on physics and statistics. In particular, we target separation structures, the linking of structures with a local semantics to global flow phenomena, and minimal representation of particle dynamics in the context of path line attributes.

Contents

Related Publications

This thesis is based on the following publications, included in part II of this thesis:

Paper A: Armin Pobitzer, Ronald Peikert, Raphael Fuchs, Benjamin Schindler, Alexander Kuhn, Holger Theisel, Krešimir Matković, and Helwig Hauser. **The State of the Art in Topology-Based Visualization of Unsteady Flow**. *Computer Graphics Forum*, 30(6): 1789–1811, 2011.

Paper B: Armin Pobitzer, Ronald Peikert, Raphael Fuchs, Holger Theisel, and Helwig Hauser. **Filtering of FTLE for Visualizing Spatial Separation in Unsteady 3D Flow**. In *Topological Methods in Data Analysis and Visualization II*, Springer, pages 237–253, 2012.

Paper C: Armin Pobitzer, Murat Tutkun, Øyvind Andreassen, Raphael Fuchs, Ronald Peikert, and Helwig Hauser. **Energy-scale Aware Feature Extraction for Flow Visualization**. *Computer Graphics Forum*, 30(3): 711–780, 2011.

Paper D: Armin Pobitzer, Alan Lež, Krešimir Matković, and Helwig Hauser. **A Statistics-based Dimension Reduction of the Space of Path Line Attributes for Interactive Visual Flow Analysis**. In the *Proceedings of the IEEE Pacific Visualization Symposium (PacificVis 2012)*, pages 113–120, Songdo, South Korea, Feb. 28–Mar. 2, 2012.

The following publications are also related to this thesis:

Paper 1: Armin Pobitzer and Helwig Hauser. **The SemSeg Project and Recent Developments in Flow Visualization**. In the *Proceedings of the Sixth National Conference on Computational Mechanics (MekIT'11)*, pages 281–292, Trondheim, Norway, May 23–24, 2011.

Paper 2: Alan Lež, Andreas Zajic, Krešimir Matković, Armin Pobitzer, Michael Mayer, and Helwig Hauser. **Interactive Exploration and Analysis of Pathlines in Flow Data**. In the *Proceedings of the International Conference in Central Europe on Computer Graphics, Visualization and Computer Vision (WSCG 2011)*, pages 17–24, Plzen, Czech Republic, Jan. 31–Feb. 3, 2011.

Paper 3: Krešimir Matković, Alan Lež, Helwig Hauser, Armin Pobitzer, Holger Theisel, Alexander Kuhn, Mathias Otto, Ronald Peikert, Benjamin Schindler, and Raphael Fuchs. **Current Trends for 4D Space-Time Topology for Semantic Flow Segmentation**. *Procedia Computer Science*, 7: 253–255, 2010.

Paper 4: Armin Pobitzer, Ronald Peikert, Raphael Fuchs, Benjamin Schindler, Alexander Kuhn, Holger Theisel, Krešimir Matković, and Helwig Hauser. **On the Way Towards Topology-Based Visualization of Unsteady Flow–the State of the Art**. In the *Proceedings of the Eurographics State of the Art Reports*, pages 137–154, Norrköping, Sweden, May 3–7, 2010.

Papers A to **D** and **Papers 1** and **4** have this thesis' author as their main author and are all written during his ph.d. project and co-authored by the principal supervisor of this thesis, Helwig Hauser.

Paper A (which is an extension of **Paper 4**) is the result of a collaborative effort within the scope of the European project *SemSeg – 4D Space-Time Topology for Semantic Flow Segmentation*, which the thesis author's Ph.D. project is a part of. The co-authors contributed to selected sections, while the main author was responsible for the classification of the papers, the overall discussion, and the general write-up of the paper.

Paper B is the result of a collaboration with Ronny Peikert and Raphael Fuchs from ETH Zürich (Switzerland), and Holger Theisel from the University of Magdeburg (Germany). The co-authors were, through discussions and feedback, involved in developing the main author's initial ideas into the methodology proposed in this paper.

Paper C is the result of a collaboration with physicists from the applied fluid dynamics group at the Norwegian Defence Research Establishment (FFI) and ETH Zürich (Switzerland). Murat Tutkun and Øyvind Andreassen, how is also this thesis' authors co-supervisor, contributed with guidance in choosing physically meaningful mathematical tools and also helped with the interpretation of the results. Raphael Fuchs and Ronald Peikert contributed with discussions on the how to apply these tools for visualization. Murat Tutkun was also involved in the write-up of the article, especially the introduction, related work, and conclusions.

Paper D is the result of a collaboration with Alan Lež and Krešimir Matković from the VRVis Research Center, Austria. This paper builds upon the results and findings of **Paper 2**, which the main author of this thesis has co-authored. He contributed to **Paper 2** by discussion and feedback to the main author, Alan Lež, mainly on the selection of attributes. Alan Lež and Krešimir Matković

contributed to **Paper D**, in turn, by discussions based on their experience with the subject. Alan Lež was also involved in the data analysis performed.

The main author of this thesis contributed to **Paper 3** with providing a discussion of his own scientific work.

This thesis is chiefly based on **Paper A** to **D**, which were worked out primarily by the thesis' author, with the help of his collaborators, as detailed above.

Part I

Synopsis

Chapter 1

Introduction

The concept of *flow* plays a crucial role in many processes in nature and industrial processes. One of the classic application areas of fluid mechanics is aerodynamics, both for the aviation and automotive industries. A design that avoids or produces certain flow phenomena can, e.g., reduce the fuel consumption of a vehicle, or increase its stability and steerability.

The underlying principles are the same in numerous other situations. Examples are fluids in and around pipe-like structures, like exhaust systems, or flexible geometries, like the human vascular system, weather phenomena and currents in the oceans, to mention but a few.

The foundation for all of those phenomena is *fluid mechanics*, i.e., the branch of physics concerned with the description of the motion of liquids and gases. A good understanding of their behavior is of great importance for many practical problems.

Historically, investigations concerning the above described phenomena have been carried out by experiment or direct mathematical analysis of the equations describing fluids in motion (Navier-Stokes equations [128]).

Experiments are one of the backbones of modern physics, but have the drawback of being usually rather costly. This is especially true for fluid mechanics. Small changes in the problem formulation can result in drastic changes in the experimental setup. For example, every change in the geometry of a vehicle in a wind tunnel experiment will require changing, or even rebuilding, the model. For complex situation this is a challenging task on its own.

The purely analytical investigation of fluid dynamics, on the other hand, is notoriously difficult. As a matter of fact, no proof (or counter-example) of the existence and smoothness of the solutions of the Navier-Storkes equations has been found yet (one of the *Millennium Prize Problems* announced by the *Clay Mathematics Institute*) [10]. In order to overcome the mathematical difficulties inherent to the governing equations, namely that closed solutions can usually not be found, analytical investigations often involve drastic simplifications in

both model and initial conditions, e.g., dimension reductions, or assumptions on irrotationality and incompressability[1].

With the advances of modern scientific computing, numerical simulation has established itself as a compelling third possibility to study fluids in motion. In contrast to experiments and analytical solutions, numerical simulations can describe almost arbitrarily complex geometries and initial conditions, and can be modified fast. Currently, numerical methods are inferior to experimental methods when highly turbulent flows around large objects should be considered (high Reynolds numbers), due to the inherent requirements on grid resolution[2].

Numerical simulations have, on the other hand, clear advantages in the study of highly time-dependent flows, i.e., flow fields with a velocity field that changes rapidly over time. Such rapidly changing fields are hard to capture in experiments due to limited time-resolution of measurement instruments.

The ability to simulate flows that change over time represents an important step towards more realistic descriptions and predictions of the underlying phenomena, and consequently the understanding of their nature. These advantages, together with the advances in high performance computing, make it highly likely that computational fluid dynamics will gain further importance in the future [84].

The shift towards computational modeling and numerical simulations in the fluid mechanics community emphasizes also the importance of the field of *flow visualization* on the informatics side. Results are not any more directly observable like in experiments or a closed formula as in analytic modeling. New means of visualizing and analyzing the, now digital, results of modeling and simulation are needed in order to fully exploit the opportunities of computational investigations. In this context, special attention has to be paid to the requirements of visualizing time-dependent flows.

1 Semantic information for flow visualization

In its widest sense, the term *semantics* is equivalent to *meaning*, and hence the semantics a visualization of fluid flow has to convey, is its physical interpretation. When using classical flow visualization techniques inspired by experimental physics, the physical interpretation is inherent to the representation. Examples for such visualization techniques with inherent semantic interpretation are arrow plots of the velocity field or particle traces. On the other hand,

[1] Examples for this practice are *potential flow* and *stream functions*, among others. Details about these solution methods can be found in Mase's textbook [128]

[2] Roughly speaking, the required grid resolution is proportional to the Reynolds number. Details can be found in the book by Durbin and Petterson Reif [30]

such techniques capture usually only an aspect of the physical process, for example instantaneous velocity and advection for the visualization techniques described above.

One of the most interesting aspects of flow visualization compared to classic experiments, is the ability to combine visual representations that are in the tradition of experimental fluid mechanics, and hence with clear interpretation, such as the ones just mentioned, with physical quantities that are not directly observable in an experiment, such as stress states or turbulence kinetic energy.

This possibility to add semantic meaning to the visualization has great potential to increase our understanding of the underlying physical phenomena as a whole, combining multiple aspects.

Additional semantic information for flow visualization can be derived in various ways, among others from the broad spectrum of physical quantities derived from theoretical considerations from continuum mechanics and statistical methods from experimental fluid mechanics.

Using the continuum mechanics toolbox [128], one has usually the possibility to choose two different view points on the physical quantities using a grid-based or particle-based description. In continuum mechanics this two concepts are referred to as *Eulerian* and *Lagrangian description* [128].

While theoretically describing the same physical process, one description may be more advantageous to capture certain aspects of the dynamics than the other. A simple example is acceleration, which is simply the time derivative of the velocity in the Lagrangian description, but becomes the material derivative in Eulerian description [128]. Classically, fluid mechanics uses Eulerian descriptors, but the increasing interest in time-dependent phenomena in flow visualization has shifted the focus towards particles, which are, in turn, the heart of the Lagrangian description of flow.

Combining appropriate Eulerian and Lagrangian representations has therefore the potential to provide semantic information that one representation only may fail to convey.

As many other physical phenomena, fluid flow has both local and non-local aspects. A local aspect is, for example, point-wise velocity, while an example for a global aspect is its transport properties. Local and global aspects are interlinked, as this examples also show. The path of a particle is, for example, defined by all velocities in the spatial locations it resides during advection. Classical flow visualization techniques target usually either local or global properties. The relation between local phenomena and the non-local process they are associated with, can also be used to provide additional semantics for local features of the flow fields.

Another possibility to add semantic information is the consideration of additional information to the flow visualization that is not captured in the underlying flow field. This situation can be seen as a particle carrying additional attributes. When storing this information for each particle for several time steps during its advection, we produce data sets that are in many ways more in the tradition of information visualization and tabular data than flow visualization and vector field data. Hence, a combination of techniques from both fields is a promising option. Such a hybrid solution of techniques in the tradition of classical flow visualization and information visualization might be referred to interactive visual flow analysis, i.e., a combination of interactive visual analysis as a general information visualization tool with flow visualization [100, 27].

Among the three just described possible ways to add semantic meaning, i.e., the combination of representations, the linking of local features to non-local phenomena they are associated with, and path line attributes, only the last one has been explored to some extent up to this point. The exchange with our collaboration partners has led to the conclusion that these are promising research directions to pursuit.

Path line attributes are already used in flow visualization, but previous experience has shown that a systematic approach to how to the selection of attributes and how to deal with large attribute sets is still missing and needed. This facilitates further exploitation of this exiting technique.

2 Overall contributions

Within the scope of this thesis, we have addressed the three options of adding semantic information for flow visualization outlined above. In particular, we have investigated

- Adding physical semantics to flow visualization based on finite-time Lyapunov exponents, by combining it with directional information. FTLE is associated to the Lagrangian perspective on fluid mechanics, while the directional information used by us is in the Eulerian frame. This work addresses therefore the combination of different representations.
- A simplification and extraction scheme that makes use of the inherent energy structure of the flow. By this technique we are able to extract features that are linked to certain dynamic processes in the overall flow. Hence, this work is along the lines of linking local- and non-local phenomena
- A condensation of a the basic set of path line attributes by statistical tools. This work is to facilitate adding semantics by path line attributes

A thorough description of the open questions addressed and the contributions made can be found in the respective sections of Ch. 3. The papers can be found in full text in part II of this thesis.

Accordingly, this thesis is structured as follows: the first part is a summary and synthetisation of the finding published in the papers worked out within the scope of this thesis' author's Ph.D. project. These papers are included in full text in part II of this thesis. They are included in their published form, but adapted to the general layout of the thesis. The respective bibliographies have been collected and updated. In Paper B we corrected an interchange of terminology[3].

The remainder of part I is structured as follows: First we review related work, based on our state of the art report (Paper A in part II) and Paper 1. Then the contributions of this thesis are discussed in more detail in Ch. 3. Next, we demonstrate the usefulness of our approaches by selected case studies. Finally, conclusions from this thesis are drawn in the concluding chapter of part I.

[3]This is commented on in more detail on the cover sheet for paper B in part II.

Chapter 2

Related Work

This chapter discusses the related work for this thesis in a summative fashion. For a much more thorough discussion, we refer to the state of the art report as included in part II (Paper A) and the related work sections in the respective papers.

In general, the aim of visualization is to convey a mental image of a phenomenon of interest by means of a visual representation and appropriate mechanisms of interaction. Although direct visualization, i.e., the immediate translation of all data items into corresponding visual elements, of all data might be possible in some cases, the level of detail in such a visualization can easily distract from the actually important information. This is especially true in the case of flow visualization, where single velocity vectors carry little information about behavior that is not observable in an isolated, point-wise fashion.

It is often much more informative to identify *coherent structures*. Such structures may be both certain regions of the computational domain, as it is the case for vortices, or particle groups that behave the same in some sense, e.g., asymptotically.

As the name already indicates, coherent structures are characterized by one or more common properties shared by all space points, or particles, that belong to them. Although similar in concept, the terminology for visualization methods based on coherent spatial structures and coherent particle group are quite different.

The first class is commonly referred to as *feature-based visualization* [162], while the latter has been referred to as visualization based on *Lagrangian coherent structures*[1] (LCS) [59]. From a computational point of view, the most interesting difference is that methods for the extraction of LCS usually involve non-local processing of the data, most prominently particle tracking. Feature-based visualization as described above, on the other hand, is usually based on local processing.

[1] This difference in terminology resembles loosely the distinction between Eulerian and Lagrangian representation in continuum mechanics [128].

1 Visualization based on features and Lagrangian coherent structures

Due to the definition of features through their properties, they are usually physically interpretable, for example resembling shock waves or separation lines. Hence, the detection of the features is often the most critical part of the visualization pipeline. For a thorough discussion of feature-based visualization techniques, we refer to the dedicated survey of this topic by Post et al. [162].

An important, but especially difficult feature class are *vortices*. Notably, there is no agreed-upon definition of vortical structures available, which is a well-known problematic in the fluid mechanics community [122], and has resulted in numerous different vortex detection schemes proposed over the years [83].

Roughly speaking, there are two different classes of methods [83]: those which detect vortices as regions in space, so-called *vortex regions*, and those which aim for the detection of the *vortex core line*, i.e., the centerline of the rotational motion.

Popular vortex region detectors are, for example, *vorticity thresholding*, *Hunt's Q criterion* [80], the so-called Δ *criterion* [14], and the λ_2 *criterion* [81]. For a discussion of the relations between these different methods we refer to Chakraborty et al. [13].

Largely used vortex core detectors are the classic methods by Levy et al. [110] and Sujudi and Haimes [193], as well as their extension for unsteady velocity fields by Fuchs et al. [40], or the "cores of swirling motion" by Weinkauf et al. [221]. Lately, two methods based on acceleration have been proposed, as well [39, 92].

When aiming at a complete classification of the flow domain (or particles), the boundaries between the distinct regions are sufficient to represent the partition. Methods yielding such partitions are often referred to as *topological methods*[2].

For steady velocity fields, dynamical systems theory provides an elegant mathematical framework for the partitioning of phase curves according to their behavior [1]. This classification is based on the analysis of *equilibria* in the dynamical system and can be found already in the late 19^{th} century in the works of Poincaré [159]. Helmann and Hesselink introduced this concept to the flow visualization community under the notion of *vector field topology* (VTF) [73, 75].

For a comprehensive discussion of VFT for two- and three-dimensional steady vector fields, we refer to Asimov's tutorial [2] and Perry and Chong [150, 151]. Essential for most visualization techniques based on VFT is the extraction of

[2] Note that these methods are not topological in a set theoretic sense. The actual geometry of the boundaries has to be considered [66].

the so-called *topological skeleton*, i.e., the equilibrium points, together with the respective invariant manifolds (separatrices), and periodic orbits as well as other critical structures. These structures constitute the boundaries of the aforementioned partition. Flow visualization techniques based on VFT have been a popular research direction and a considerable amount of literature is available on the topic. For further reading we refer the reader to Sec. 2 in Paper A and the dedicated surveys of Scheuermann and Tricoche [182] and Laramee et al. [106].

As already mentioned, VFT is based on the analysis of equilibrium points (often also *critical points*). This analysis assumes *isolated* critical points in systems of *autonomous* ODEs, e.g., the equations defining trajectories in flow fields. These assumptions make it inapplicable to time-dependent velocity fields, since they are non-autonomous, or, when looking at the problem in $(n+1)$ dimensions[3], have no isolated critical points. Practical examples for the deficiencies of VFT when applied to unsteady flows have been given recently [184, 227].

Nevertheless, VFT is still an important inspiration since an optimal solution for unsteady flow fields should lead to comparable results. One of the most prominent properties of the segmentation obtained from VFT is the extraction of lines or surfaces representing the stable and unstable manifolds, so-called *separatrices*. These separatices confine regions of phase curves with homogeneous properties with respect to their asymptotic behavior. The analogous structures for non-autonomous dynamical systems are referred to as *Lagrangian coherent structures* (LCS) [58].

Although the concept of LCS as boundaries of particle groups with similar behavior is rather intuitive, no strict mathematical definition is available. One of the most prominent ways to define LCS is related to *finite-time Lyaponov exponents* (FTLE), a separation measure inspired by stability theory [50]. More precisely, ridges of this scalar separation measure have been proposed as LCS [60, 184].

Ridges of the FTLE field act asymptotically as transport barriers in the flow and are crossed by a small amount of particles only. This amount is inversely proportional to the integration time, i.e., ridges converge to material lines [184]. Hence, FTLE ridges can be seen as a weak analogon of invariant manifolds for autonomous systems. This property makes the use of such ridges appealing for the purpose of unsteady flow visualization and a considerable amount of effort has been made to efficiently compute and extract them (cf. Sec. 4 and 6 in Paper A). It is worth noting, however, that recent work of Haller [62] shows that LCS and FTLE ridges can not be identified, giving examples of dynamical

[3] The spatial dimensions and time. The transformation from an non-autonomous system to an autonomous system in higher dimensions is achieved by canonical lifting (cf. Sec. 5 in Paper A).

systems where observable LCS are not FTLE ridges and vice versa [62]. Also examples given in Paper B show that FTLE can fail to identify observable separation structures.

Further details about the computation of FTLE and related maps are provided in Sec. 1 of Ch. 3, along with a more detailed description of the physical interpretation.

2 Interactive visual analysis in the context of flow analysis

VFT-based visualization methods are usually automatic methods, i.e., the result is dependent on the data and the chosen algorithm only. This means that the user has little influence on the output. One of the advantages of such methods is that the visualization is consistent, independent of the proficiency of the user. In the case of flow visualization, on the other hand, we usually deal with expert users. Hence, allowing for an interactive integration of their knowledge about fluid dynamics in general, and the data set under examination in particular, in the process of generating the visualization is a promising complementary approach.

The concept of *interactive visual analysis* (IVA) combines automated analysis steps with the user knowledge in a feedback loop, allowing for iterative result optimization [94]. IVA is quite common in fields like economics, but by no means restricted to them, as recent results in flow visualization show [29, 100, 131, 105]. Besides the fact that domain knowledge is exploited, the main appeal of this approach is the possibility to obtain a flexible segmentation that can be adjusted to the situation the specific data set describes, taking also other information than just the velocity field itself into account.

Even though data sets describing flow phenomena are usually two- or three-dimensional (plus time, in the case of unsteady velocity fields), other information (e.g., pressure, density, temperature, ...) needs to be exploited, when available. Even if the velocity field is given alone, often derived fields are calculated to analyze the flow (vorticity, λ_2, ...), especially in the context of feature extraction described above.

This yields data sets with high dimensionality that need to be analyzed. As already outlined above, the automatic analysis of these additional dimensions has the drawback that the knowledge of a domain expert operating the visualization tool is not exploited. Additionally, it is often unclear how such an automated analysis should look like.

IVA is a theoretical visualization framework based on the idea to depict multiple dimensions in multiple view, using, e.g., histograms and scatter plots. These views, showing the data consistently but in different representations and different dimensions of them, are dynamically linked and selecting a certain data range in one view highlights the corresponding data values in the other views. Multiple selections in all views can be combined and related to each other by logical "and" and "or" connection. In this way, complex queries can be formulated for the data and interactively refined. In the context of flow visualization, usually a three-dimensional view of the physical domain is included to ease the spatial location of the investigated properties. For the description of a IVA framework for flow analysis in general, and the framework this ph.d. project has been carried out in, in particular, we refer to Doleisch [24].

Bürger et al. [7] use IVA to analyze vortical motion. One of the challenges in the task of identifying vortical motion is that no agreed-upon mathematical definition of such motion exists. They authors show how the combination of multiple vortex detectors in an IVA framework can both enhance and robustify the identification of vortices. Furthermore, they use additional measures to distinguish, e.g., slowly rotating vortices from fast rotating.

In the context of time-dependent velocity fields, the analysis can be conducted adopting a Lagrangian perspective on the flow. Computing particle trajectories, both global properties of the trajectory itself (average velocity, winding angle, arc length,...) and other values along the trajectory (curvature, torsion, particle velocity) can yield interesting insight in the dynamical behavior. Shi et al. [186] describe the use of IVA in this context. They investigate a large number of *path line attributes*, finding that for most questions investigated the examination of a rather small subset of those seems sufficient. A formal definition of path line attributes is provided in Sec. 1 of Ch. 3.

Lež et al. [112] show how a multi-step analysis can be used to speed up path line-based IVA of unsteady velocity fields. They propose to seed particles on a relatively coarse grid first and identify possibly interesting areas in this path line data set, before starting the full resolution path line analysis in this regions only. Additionally to the selection of certain path lines by their attributes, the authors propose direct path line brushing (i.e., "marking up" of certain path lines), using projection views.

3 Chapter summary and conclusions

We see that flow visualization has, up to the current point, to a large extent dealt with detecting and visualizing structures with a clear predefined semantic meaning, as vortices or LCS. The reverse process, namely visualization tech-

niques that provide a semantic interpretation that are not per definition associated with the extracted structure, is a currently not very extensively explored research direction.

The research direction of path line attributes is perhaps the most visible in this context. While clearly a considerable amount of good work has been done in this direction, the crucial aspect of the selection of attributes has not been addressed yet.

These two observations can be seen as a starting point and motivation for the research presented in the following chapters of this thesis.

Chapter 3

Physics- and Statistics-based Semantics

In this chapter we discuss the contributions of this ph.d. work in a detailed manner. We introduce briefly the problems we address, and discuss our work on the problem on a conceptual level. Technical details are left to the respective full papers in part II.

Before the actual discussion of the contributions in Sec. 2, a short outline of some of the fundamental concepts for this work is given.

1 Foundations

For the time being, we assume to have a flow given by its velocity field. This velocity field is discrete and stored on a grid covering the computational domain. For all data sets used in this thesis, those velocity fields originate from numerical simulations or are originally analytic and sampled on a grid. Hence, the data is given as two- or three-dimensional vectors, stored in specific space point, and possibly also varying in time. If not defined otherwise, we denote the velocity field by

$$\mathbf{v} : (\mathbf{x}, t) \mapsto \mathbf{v}(\mathbf{x}, t) \tag{3.1}$$

where $\mathbf{x}$ and t are specific points in space and time, respectively.

1.1 Path lines and flow map

A *path line* is the trajectory of a massless particle, advected by the velocity field. Formally, the path line $\mathbf{x}$ of a particle that resides in the position $\mathbf{x}_0$ at time $t = t_0$ is given by the following initial value problem of the ordinary differential equation

$$\frac{\mathrm{d}\mathbf{x}}{\mathrm{d}t}(t) = \mathbf{v}(\mathbf{x}(t), t), \quad \mathbf{x}(t_0) = \mathbf{x}_0 \tag{3.2}$$

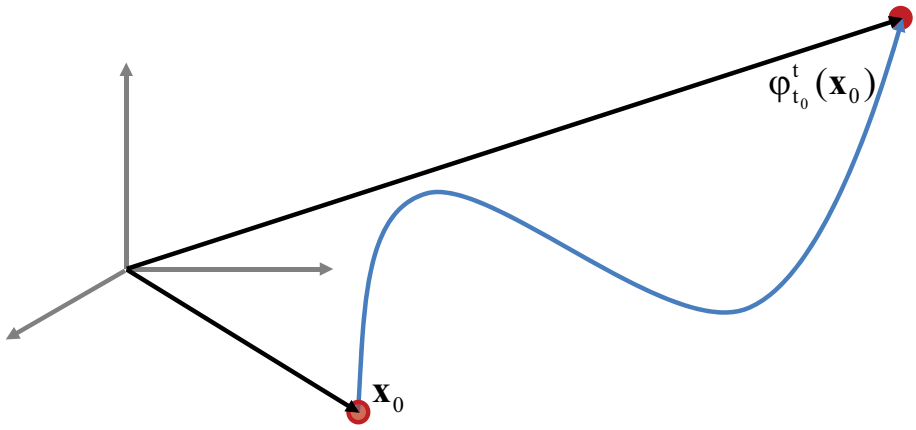

Figure 3.1: Illustration of the concept of the flow map. The exact path of the particle between start and end point is not captured in the mapping.

or, in integral form,

$$\mathbf{x}(t) = \mathbf{x}_0 + \int_{t_0}^{t} \mathbf{v}(\mathbf{x}(\tau), \tau) \mathrm{d}\tau \tag{3.3}$$

which gives the position of the particle at time t.

The function that maps a particle's position at time t_0 to its position at time t is usually referred to as *flow map* and denoted by

$$\varphi_{t_0}^{t} : \mathbf{x}_0 \mapsto \mathbf{x}_0 + \int_{t_0}^{t} \mathbf{v}(\mathbf{x}(\tau), \tau) \mathrm{d}\tau \tag{3.4}$$

It is worthwhile noticing that no information on the path between $\mathbf{x}_0$ and $\varphi_{t_0}^{t}(\mathbf{x_0})$ is contained in the mapping[1]. Fig. 3.1 illustrated the concept.

1.2 Flow map gradient, Cauchy-Green strain tensor

Given a fixed integration time and the respective flow map, the classification of the particles into coherent groups can be of interest. The boundaries of such groups are often referred to as *Lagrangian coherent structures* (LCS). According to whether or not particles are converging or diverging from those boundaries, they are said to be attracting or repelling.

The relative converging or diverging behavior of particles can be interpreted as deformation of the continuum between them, and is therefore related to the

[1] $\varphi - id$ is also known as the *displacement field*.

material deformation gradient known from continuum mechanics. The material deformation gradient is indeed the gradient of the flow map

$$F_{ij} = \frac{\partial \varphi_i}{\partial x_j} \tag{3.5}$$

As every non-singular symmetric tensor, we may use the so-called *polar decomposition* to isolate rotation and stretching. If we are interested in the strain in the direction with respect to the undeformed material, we choose the *right* polar decomposition, i.e., stretching first and then rotation[2].

Every rotation is isometric, therefore the relevant information for convergence and divergence is contained in the stretching. This stretching information is captured in the so-called *Cauchy-Green strain tensor*

$$C_{ij} = \sum_k F_{ki} F_{kj} \tag{3.6}$$

or in matrix notation, using $\mathbf{F} = \mathbf{RS}$, where $\mathbf{R}$ is the rotation and $\mathbf{S}$ the stretching matrix described above, we get the following equality

$$\mathbf{C} = \mathbf{F}^T\mathbf{F} = (\mathbf{RS})^T \mathbf{RS} = \mathbf{S}^T\mathbf{R}^T\mathbf{RS} = \mathbf{S}^T\mathbf{S} \tag{3.7}$$

While the polar decomposition is not needed for the actual calculation, it shows that the Cauchy-Green strain tensor indeed disregards the rotational information. Intuitively, the tensor describes the deformation of a infinitesimal small sphere around a particle.

For a more thorough discussion of the material deformation gradient, Cauchy-Green strain tensor, and related concepts we refer the reader to Mase's text book on continuum mechanics [128].

1.3 Finite-time Lyapunov exponents

As explained in the previous section, the Cauchy-Green strain tensor is related to the deformation of a infinitesimal small sphere. If only the distinction between divergent and convergent behavior is of interest, we have to consider only the magnitude, not the direction of the relative stretching. The maximal rate of deformation the sphere undergoes is given by the largest eigenvalue of

[2]The decomposition in reversed order is also possible. In that case the stretching of the material is represented in the so-called *spatial*, or *Eulerian* reference system. The difference between spatial and material reference system are discussed in more detail in the discussion section of Paper B in Sec. 2 of this chapter. For additional reading on the topic we refer to Mase's textbook on continuum mechanics [128]

the Cauchy-Green strain tensor. Assuming that the size of an infinitesimal displacement d$\mathbf{x}$ grows exponentially over time with a constant rate, i.e.,

$$||\varphi_{t_0}^t(\mathbf{x}+\mathrm{d}\mathbf{x}) - \varphi_{t_0}^t(\mathbf{x})|| \propto \exp\left(\epsilon(t-t_0)\right)||\mathrm{d}\mathbf{x}|| \tag{3.8}$$

we get the maximal rate of deformation as

$$\begin{aligned}\epsilon &= \frac{1}{|t-t_0|}\log\left(\max_{||\mathrm{d}\mathbf{x}||=1}\frac{||\varphi_{t_0}^t(\mathbf{x}+\mathrm{d}\mathbf{x}) - \varphi_{t_0}^t(\mathbf{x})||}{||\mathrm{d}\mathbf{x}||}\right) = \\ &= \frac{\log\left(||\mathbf{F}||_{op}\right)}{|t-t_0|} = \frac{\log\left(\sqrt{\lambda_{\max}\left(\mathbf{C}\right)}\right)}{|t-t_0|}\end{aligned} \tag{3.9}$$

where $||-||_{op}$ is the *operator norm* and $\lambda_{\max}(-)$ the maximal eigenvalue of a tensor. ϵ is usually referred to as the (maximal) *finite-time Lyapunov exponent* (FTLE). The equalities in eq.(3.9) follow directly from expanding φ in a Taylor series and the definition of the operator norm [51]. Details can be found in Paper B, Sec. 3.

FTLE is a popular detector for LCS. For details we refer to Haller [59], who proposed FTLE for the detection of LCS first, and Shadden et al. [184].

1.4 Path line attributes

Another recurring term in this thesis is *path line attribute*. Such a path line attribute is a mapping that depends a specific path line $\mathbf{x}(t)$ and its time parameterization. Path line attributes describe properties of the respective particle over time, and are hence most conveniently formulated in the *Lagrangian* or *material* frame of reference. Formally, we can express any (scalar of vector valued) path line attribute A as

$$A : (\mathbf{x_0}, t) \mapsto A(\mathbf{x}_0, t) \tag{3.10}$$

where $\mathbf{x}_0$ is the position of a certain path line at seeding time, and hence an unique identifier of the path line.

In this context, it is a known problem that adding too many attributes to investigate may actually make the analysis more challenging. Hence, the originally present information should be expressed in an as compact as possible manner. In other words, a minimal attribute set describing the flow dynamics is of particular interest.

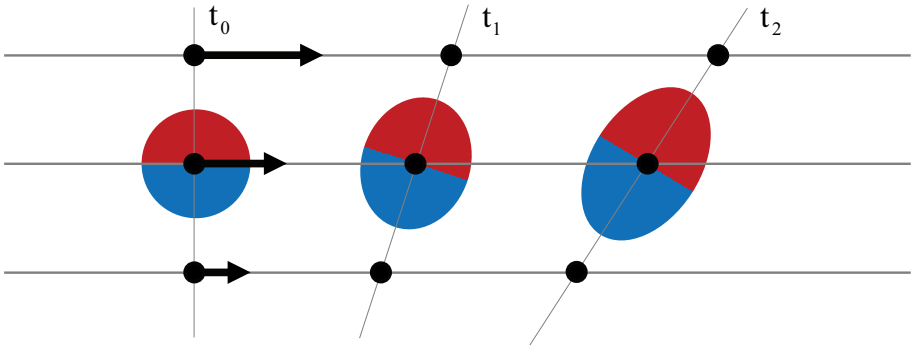

Figure 3.2: Illustration of the concept of the flow map. The exact path of the particle between start and end point is not captured in the mapping.

2 Contributions

After the introduction of some basic concepts and mappings, we now discuss the contributions of this thesis. The chapter is organized according to the type of contribution, as outlined in the introduction.

2.1 Combination of representations

Problem Statement

As already explained in Sec. 1 of this chapter, the FTLE field gives only information on the maximal rate of stretching, disregarding the direction of this maximal stretching. It is intuitive that particles moving in different directions will induce high FTLE values. However, particles moving in the same direction with different speeds, like it occurs in shear layers, are also associated with high FTLE values. To illustrate this, we use a simple thought experiment (the same as in Paper B).

We consider two particles that travel on straight parallel lines with constant velocity, but the one velocity being larger than the other. At a certain time, these particles have a certain distance from each other. The distance between the particles increases monotonically (due to the different particle velocities), but their paths remain nonetheless parallel, leading the particles into the same area (but at different times).

Fig. 3.2 illustrates the described separation. In general, all particles traveling along locally parallel paths, but at different speeds, introduce high FTLE val-

ues. Informally, we may speak of separation due to different velocity directions and different velocity magnitudes.

Contributions

Within the scope of Paper B, we propose a measure that enables the distinction between high FTLE values due to the two different "types" of separation captured by high FTLE values, described in the problem statement.

Intuitively, the qualitative difference between the separation due to different velocity directions and velocity magnitudes is the *direction* relative to the path line in which the separation occurs. This information is not contained in the FTLE value. The Cauchy-Green strain tensor, on the other hand, also includes a directional information of the stretching. This stretching information is, however, with respect to the unrotated state at the seed point of the particle x_0, i.e., the material before the deformation, and not related to the spatial configuration of the deformed object or the direction of the path line.

If we want to quantify the stretching in the deformed material, i.e., the spatial directions of the of the strain, the deformation can be written as rotation first and then stretching. This is formally equivalent to the left polar decomposition of the material deformation gradient, or flow map gradient, i.e,

$$\mathbf{F} = \mathbf{TR} \tag{3.11}$$

where $\mathbf{R}$ is a rotation, and $\mathbf{T}$ represents stretching as described earlier. It is important to notice that this stretching is *not* the same as the one in Eq. (3.7). Fig. 3.3 illustrates this. Finally, we can extract the spatial strain direction associated with the FTLE value as the eigenvector associated with the largest eigenvalue of $\mathbf{FF}^T$[3]. This direction is with respect to the particle after advection, and can be compared to the direction of the path line.

The direction of the path line in $\mathbf{x} := \varphi_{t_0}^t(\mathbf{x}_0)$ is the velocity $\mathbf{v}(\mathbf{x}, t)$. Hence, the angle between the spatial strain direction associated with the FTLE value, and the path line velocity is a good measure for how much of the "separation" occurs along the path line. We propose the integral over the unsigned cosine of the angle as a measure for the diverging behavior from a given path line.

By a carefully chosen sample rate and a correction factor for isotropic strains we are able to robustify our measure. The final measure is given by Eq. (11) in Paper B.

[3] Alternatively to the polar decomposition, one may also use the *singular value decomposition* (SVD) to derive the same geometric intuition. From this decomposition it is also clear that $\mathbf{C}$ and $\mathbf{FF}^T$ have the same eigenvalues, but, as already derived, not the same eigenvectors. The derivation in Paper B follows these lines, and is equivalent to the here given.

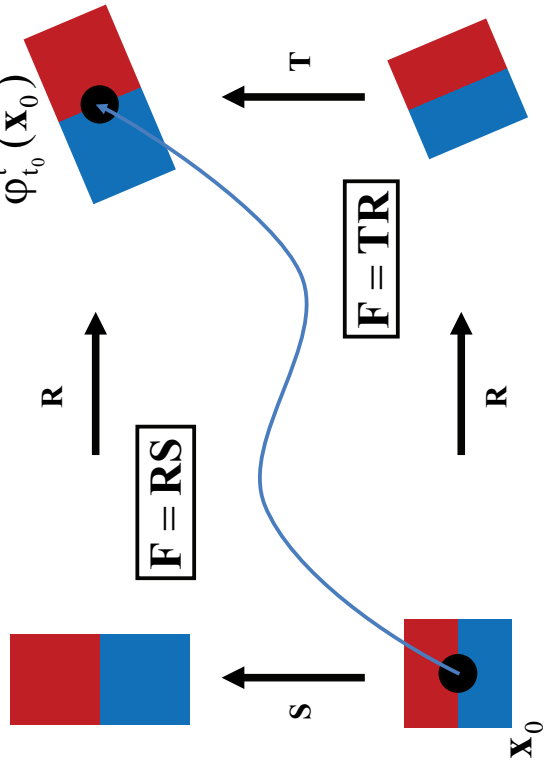

Figure 3.3: The two possible polar decompositions of the material deformation gradient **F**. We see that the directions in which the stretching acts change depending on whether it is executed before the rotation or after, even though they describe the same deformation (given by **F**). The difference is whether we are interested in the straining directions regarding the undeformed material or the straining directions regarding the spatial configuration of the deformed material. The first directions are referred to as the *material strains*, the latter as the *spatial strains* [70].

We show by analytical examples and data sets from computational fluid dynamics that our measure is indeed able to distinguish between the two types of separation described in the problem statement. We are also able to show that there are observable separation structures that are not detectable by FTLE (in situations with constant FTLE fields), but our separation measure is able to detect. This result suggests that the identification of high FTLE values and separation is not correct. Recent results by Haller [62] suggest this as well.

It is worthwhile noticing that both the Cauchy-Green strain tensor $\mathbf{C} = \mathbf{F}^T\mathbf{F}$ and $\mathbf{F}\mathbf{F}^T$ describe the same strain involved in the deformation given, but in different reference frames. The first expresses the strain with respect to the particle configuration at seeding time t_0, which is commonly referred to as the material axes, and is hence a *Lagrangian descriptor* of the strain. The latter, on the other hand, expresses the strain with respect to the current particle configuration at time t, which is usually referred to as the spatial axes. This makes it an *Eulerian descriptor* of the stain.

Our measure is an example of how the combination of Lagrangian descriptor of the deformation, namely the material deformation gradient, or flow map gradient, combined with an Eulerian representation of strain involved in this deformation, namely the principal spatial strain direction, and can be used to add further semantic meaning to the FTLE field.

The details about the derivation and exact formulation of the separation measure and its practical computation can be found in Paper B included in part II of this thesis.

2.2 Linking of local and non-local phenomena

Problem Statement

One of the properties that make numerical simulations so compelling is that, if enough computation power is available, the flow can be quantified to the finest level of detail. This gives the opportunity to investigate the behavior of the flow at these scales, instead of using models.

For general extraction methods targeting coherent structures, data sets containing such complex, fine scale flow configurations tend to produce somewhat dense outputs. This can, in turn, cause difficulties to interpret the data making use of visualization tools. Therefore, methods able to remove details that are adding complexity to the visual output, while being unimportant under certain aspects, are of great use.

In general, the problem can be approached from two sides. Either we extract all coherent structures according to a certain detection scheme and remove

some of them afterwards, or we simplify the velocity field and apply feature extraction afterwards.

The first approach is usually applied in the context of *feature-based flow visualization*. The criteria for discarding a feature are typically of a geometric nature, like length, area and volume of features, or their reciprocal distance [170, 77]. This approach obviously serves the purpose of reducing the visual clutter well. On the other hand, it is unclear how the visual output refers to the original velocity field. Hence, semantic information extracted from these visualizations may not correspond to the semantics of the original field.

Similar approaches have been used for the simplification of topological skeletons, where critical points have been collapsed if their reciprocal distance is small [19], they cancel each other [210], or are not persistent over time [198].

Simplifying the velocity field directly, avoids the problem of correspondence between the semantics conveyed by visual output and the semantics of the underlying data. However, manipulating the velocity vector values is not unproblematic. It is, for example, known that simple low pass filtering (i.e., smoothing) affects both time and length scales of the flow [216]. In other words, low pass filtering changes the semantics of the flow field in question. The same is true for methods based on vertex removal or edge collapsing as the one proposed by Dey et al. [23]. Those methods are local, in the sense that they take only velocity information in a small neighborhood in consideration, and neglect the connection to larger-scale characteristic patterns in the flow field.

A extraction scheme for coherent structures, that allows for simplification, while capturing the semantics of the simulated (or measured) flow at a chosen simplification level is missing.

Contributions

Within the scope of Paper C, we propose a physics-based simplification scheme for velocity fields for both feature- and LCS-based flow visualization techniques. Furthermore, we discuss the impact of the simplification on particle advection, which is the base of many classic flow visualization techniques, like path lines.

Conceptually, simplification can be seen as removal of details that are below a certain "significance threshold". In image processing, for example, this may translate in the removal of small objects. In order to perform the removal in this example, we need to identify the objects and estimate their importance, in this example size, first.

In the same fashion as an image may be though of consisting of different object,

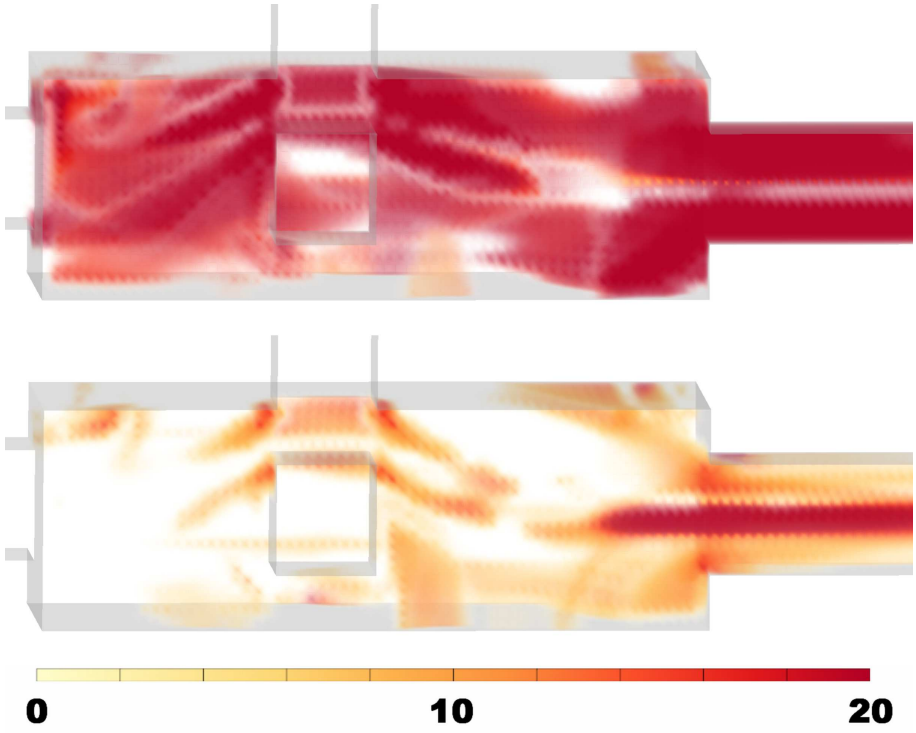

Figure 3.4: Vorticity based feature extraction based on the original field (top) and as simplified field (bottom), respectively. We see a strong reduction of the structures in the back of the top picture when taking the most dominant modes only. In the outflow, the vorticity field based on the most dominant modes reveals one instead of two vortices. For further discussion we refer to Paper C.

flow fields, in particular turbulent flows, consist of different *scales of motion*. These scales range from flow patterns that drive the large scale motion of the fluid to the finest scales where the kinetic energy is dissipated to internal heat. It is important to notice that these scales are of global nature, i.e., all of them influence the whole flow domain. In fact, the flow field is a superposition of the different scales of motion [144], which are velocity vector fields themselves.

As in the image processing example, simplification can be achieved by removing objects, in this case scales of motion, that are considered "unimportant". The contribution of the single scales to the flow field in total can be characterized by the amount of energy they carry. The different scales of motions are in fact connected to the so-called *turbulence energy cascade*, i.e., the different stages of the dissipation of kinetic energy from the mean flow to the finest scales. The

turbulence kinetic energy (TKE) contained in every scale of motion is therefore a canonic measure of the "dominance" of a scale in the flow [123]. Due to this inherent relation between the scales of motion and the turbulence energy cascade, these scales are often also referred to as energy-scales.

In order to extract the different energy-scales and their TKE, we make use of the *proper orthogonal decomposition* (POD). The theoretical background, the practical computation, and properties of the POD are discussed in Sec. 3 in Paper C. The most important property for our purpose is that any time step of the original flow field has a unique representation as a linear combination of the energy-scales, which allows us to easily remove unimportant energy-scales from the time step.

According to this outline, our simplification and extraction scheme consists of the following steps:

1. Computation of the energy-scales
2. Simplification of the flow field, removing scales with low TKE content
3. Application of a standard extraction scheme

We investigate the impact of our proposed scheme by applying it different standard extraction schemes and data sets. We see that we are able to

- Achieve considerable reduction of the visual clutter in the output while preserving dominant structures
- Uncover features that are "hidden" by low TKE energy-scales
- Achieve a denoising effect for LCS extraction based on FTLE

Fig. 3.4 illustrates the first two effects on the example of vorticity thresholding. The data set describes flow through a T-junction with an internal obstacle with inlet from the top and left. The result from the standard extraction is shown in the top image and the result from our proposed extraction scheme in the bottom. For further description of the data set, the vorticity thresholding and discussion of the results, we refer to Paper C.

In order to explain the third effect, we investigate the error introduced by the simplification on particle advection. We find that the error is of an order of magnitude that allows the combination of POD-based simplification and integration without considerable loss of precision. The same deblurring effect observed by us, has also been described by Kourentis and Konstantinidis [102] in parallel to the here presented work.

Our focusing on energy-scales that are associated with large scale motion yields also a semantic information not deductible from the original structures, namely their role in the overall dynamics of the flow. Our extraction scheme links the visible structures directly to the energy-scales they live on.

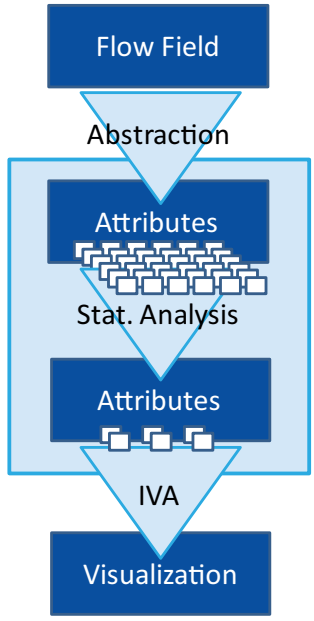

Figure 3.5: The Figure illustrates the idea behind the condensation of the set of path line attributes. We single out representative path line attributes with the help of statistical tools. The reduced path line attribute set is then used for the interactive visual flow analysis. For the discussion of the benefits of such a reduced path line attribute set, we refer to Sec. 2.3 in this chapter.

Further detail about the algorithmic details, discussion of local error of the simplification, integrative error and the results can be found in Paper C.

2.3 Condensation of path line attributes

Problem Statement

As noted in the introduction, the enrichment of particle traces with additional attributes and the analysis of these so-called *path line attributes* by means of interactive visual analysis (IVA) has great potential to yield a better semantic of the flow field than the analysis of the particle traces alone. This has been shown in work by Bürger et al. [7], Shi et al. [186], and Lež et al. [112], among others.

While the results of previous works are more than convincing, the actual selection of appropriate attributes is an unanswered question, although this question

is crucial for a successful application of path line attributes. In the context of IVA it is known, that a systematic exploration of data sets gets more and more challenging, the more dimensions (in our case attributes) have to be considered. Hence, the selection of an as small as possible attribute set, is an important task to enable efficient analysis. Therefore, the adding of further path line attributes has to be considered carefully.

Roughly speaking, we can distinguish between additional attributes that are directly derived from the flow field in question (e.g., vorticity, acceleration,...), and attributes related to additional quantities of importance for the simulated situation (e.g., density, temperature,...). The latter type of attributes is in general not available, also because these effects are not always of importance, for example for incompressible flows. In other situations, like combustion processes, they may play an important role.

The first type of attributes, i.e., those derived from the velocity field, are usually well-known feature detectors. Feature detection and extraction has been a very active research topic in both the physics and flow visualization community, and hence a large number of possible interesting attributes derivable from the velocity vector field is available [162, 83, 186, 174]. Many of them target, however, the same semantic (most prominently, vortical flow and vortex detectors, cf. [83]), which introduces possible redundancy when considering all of them. Apart from the redundancy in information, considering multiple descriptors that essentially target the same behavior can also introduce a large overhead in computation time and storage.

These considerations imply that the condensation of the set of possible attributes is a promising approach for the attributes derived from the flow field. The restriction of the condensation to this first type of attributes is also necessary, in order to yield a generally usable condensed attribute set for interactive flow analysis. Fig. 3.5 illustrates the concept of the condensation.

Contributions

Within the scope of Paper D, we propose a set of path line attributes, that captures the underlying physical properties of the flow field with as little redundancy as possible.

In order to identify such an path line attribute set, we compute first a large number of different path line attributes that have been used successfully in the literature. Then we apply a statistical dimension reduction technique, namely *exploratory factor analysis* (EFA) [190] in order to identify the intrinsic dimensionality of the space spanned by the path line attributes.

EFA yields not only the dimensionality of the space, but also how the original

variables are related to the (unknown) statistical variables that span the space, called *factors*. In this way, we are able to single out a set of the attributes that represent the whole attribute space best possible. The choice of the statistical tool and further algorithmic choices in the analysis are detailed in Sec. 1 and Sec. 3 of Paper D, respectively.

Since we are aiming at finding a set of path line attributes that is generally usable for interactive flow analysis, this procedure is performed for several CFD data sets and an analytic vortex model. These data sets span a variety of different geometries, simulation types, and application areas in order to make sure that recurring patterns in the representative path line attributes are not induced by the specific simulation setting, but indeed more general.

We find that on average six factors are needed to represent the whole data set, and identify the path line attributes related to these factors. The attributes found are:

- Quadratic statistical invariants [116]
- λ_2 [81]
- Velocity
- Average speed along the path line
- Particle position
- Start to end distance of the path line

An overview over the outcome of the statistical analysis for every single data set can be found in Table 1 in Paper D.

A confirmatory statistical analysis shows that these attributes account on average for 95% of the data complexity. It is worthwhile noticing that the first attribute refers to the shape of the particle path[4], while the second is related to swirling motion. The remaining attributes are related to the dynamic behavior of the particles. This may yield additional intuition during the analysis. The attribute set is self-contained in the sense that all quantities are derivable without the computation of auxiliary attributes, like vorticity.

For details about how we identify the characteristic attributes we refer the reader to Paper D.

[4] The quadratic statistical invariants are indeed shape descriptors of space curves and used for shape recognition [116]

Chapter 4

Demonstration

This chapter exemplifies the application of the techniques described in the previous chapter by selected case studies. The examples are organized according to the type of semantic enhancement they are related to. For further examples we refer the reader to the demonstration sections in the respective papers.

1 Combination of different flow representations

As explained in Sec. 2.1 of Ch. 3, there are two different types of particle separation that FTLE captures: separation due to differences in velocity direction and differences in velocity magnitude. We will give two examples of situations where our separation measure can be used so gain a better understanding of the semantics of the underlying velocity field.

1.1 Filtering of FTLE fields by the separation measure

If we want to neglect FTLE values that are due to differences in particle speed, our separation measure can be used as a threshold-type filter. In the IVA framework we use, this filtering is easily accomplishable by brushing the desired data range in an appropriate data view, e.g., a histogram or a scatter plot.

We apply this technique to the simulation of a breaking dam illustrated in Fig. 4.1. The main flow currents are illustrated in Fig. 4.1(a), Fig. 4.1(b) shows a FTLE field where values under a certain threshold are rendered transparently.

We can identify several structures that are to be expected from the main currents, e.g., in front of the obstacle, separating flow that passes the obstacle and flow that recirculates in front of it. The large region of high FTLE values in the upper left, on the other hand, is possibly due to shearing.

In Fig. 4.2 we see a close-up of the region in question. The top image shows the unfiltered field, while the bottom images shows the field after removing regions

(a) Schematic overview (b) FTLE field

Figure 4.1: (a) Schematic overview over the flow domain, z being the streamwise direction. (b) A FTLE field of a simulation of a bursting dam. The FTLE values lower a certain threshold are rendered transparently. We see that we can identify expected structures around the obstacle. The upper rear part of the flow domain shows large regions with high FTLE values, presumably induced by shearing.

where our separation measure is lower than a certain threshold. Path lines have been added to confirm that we really remove values which represent no spatial separation (cf. region A), and leave regions with high spatial separation untouched (cf. region B).

For further examples of the application of our technique, we refer to Paper B.

1.2 Application to regions of constant FTLE

We give an example of an analytically defined two-dimensional vector field with *constant* FTLE field, but a clear spatial separation. The field is given by

$$\mathbf{v}: \quad (x, y) \mapsto (x - 1, 1)^T \tag{4.1}$$

Obviously, all particles seeded at positions with an x-coordinate smaller than 1 travel to the left, while those seeded at positions where the x-coordinate is larger than 1 travel to the right. Since the FTLE field is constant, the separation line at $x = 1$ can not be detected by this method. Our proposed separation measure, on the other hand, is able to capture this behavior, as shown in Fig. 4.3.

2 Linking of local- and non-local features

In the previous chapter we have discussed that the removal of scales with less turbulent kinetic energy allows us to focus on structures that are related to the dominant scales of motion. The knowledge about this link to certain scales of motion helps us to better understand the semantic meaning of those structures.

We apply our simplification and feature extraction scheme to FTLE computation in the direct numerical simulation of a turbulent channel flow at frictional

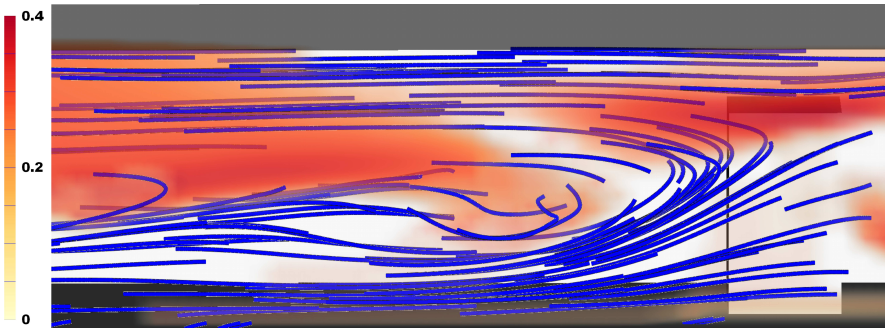

(a) FTLE field

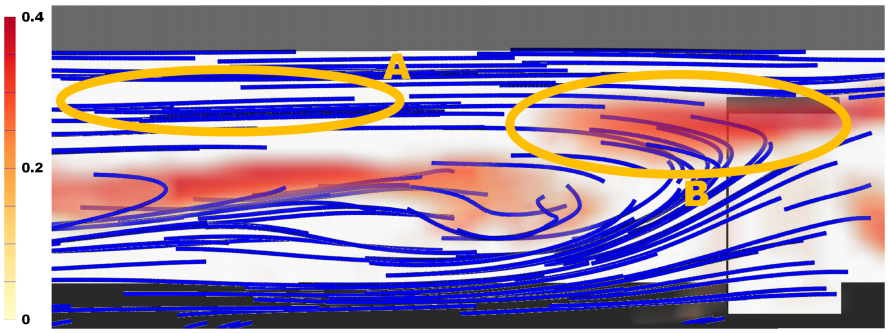

(b) filtered FTLE field

Figure 4.2: A cross section of the (a) FTLE and (b) filtered FTLE field. The ellipse (A) shows a region where the filter has a strong impact. We see that the path lines are locally parallel and show little to no spatial separation. In contrast, we see that the structure below the ellipse separates path lines moving from the left to the right (above) from those moving in the opposite direction (below). In the same fashion, the ellipse (B) indicates a structure that separates particles coming from the left and passing over the obstacle, from those moving back to the left end of the flow domain. This structure is persistent under our proposed filter. For details about the parameter settings in the FTLE calculation and the filtering we refer to Paper B.

Reynolds number $Re_\tau = 180$. We extract the FTLE field from both the original velocity field and for simplified fields based on the two and four most dominant scales of motion.

When extracting the FTLE from the two most dominant scales of motion only, we get more crisp structures. Low turbulence kinetic energy scales seem to add noise to the computation, while not carrying additional information. Adding two more scales, on the other hand, does not change the output of the FTLE

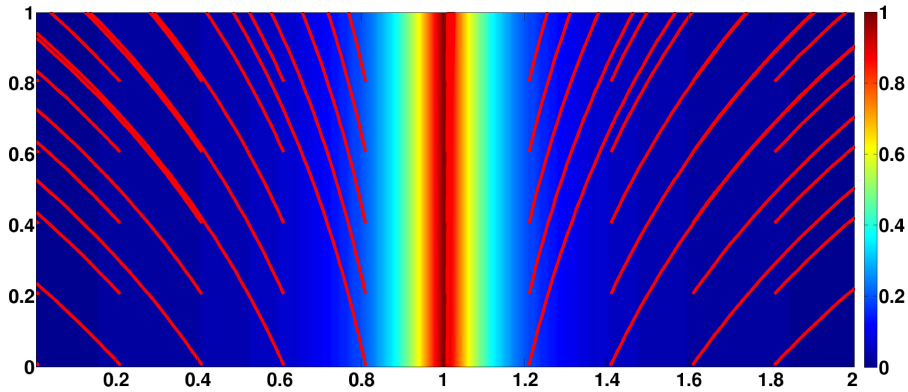

Figure 4.3: Our separation measure in a vector field of constant FTLE values. The path lines show a clear spatial separation of the particle seeded to the left and to the right of the line $x = 1$. This illustrates that there are observable separation structures that FTLE is not able to detect. Our separation measure, on the other hand captures this structure. For further details and additional examples we refer to Paper B.

computation. Hence, we can conclude that those structures are indeed linked to the very largest scales of motion only.

Since FTLE is based on particle advetion, which is in turn driven by the scales responsible for the transport in the flow, this is in full accordance with the physical intuition behind the turbulence energy cascade. Similar conclusions have also been drawn by Kourentis and Konstantinidis [102]. The authors apply a similar simplification scheme to FTLE computations for experimental data.

3 Condensation of path line attributes

In order to demonstrate that interactive visual flow analysis based on the reduced path line attribute set proposed by us is equally expressive as the analysis based on the full attribute set, we compare results from a previously published case study by Lež et al. [112] to the results our analysis can achieve on the same data set.

The target application in this case study is the design of an exhaust manifold system. More precisely, the occurrence (and possibly, origin) of *back pressure* in the exhaust pipes is investigated. Back pressure is known to affect the performance, in particular power and fuel consumption, negatively. Detecting this behavior is a first step towards optimizing the design.

Fig. 4.5 gives an overview of the geometry and path line behavior for this case

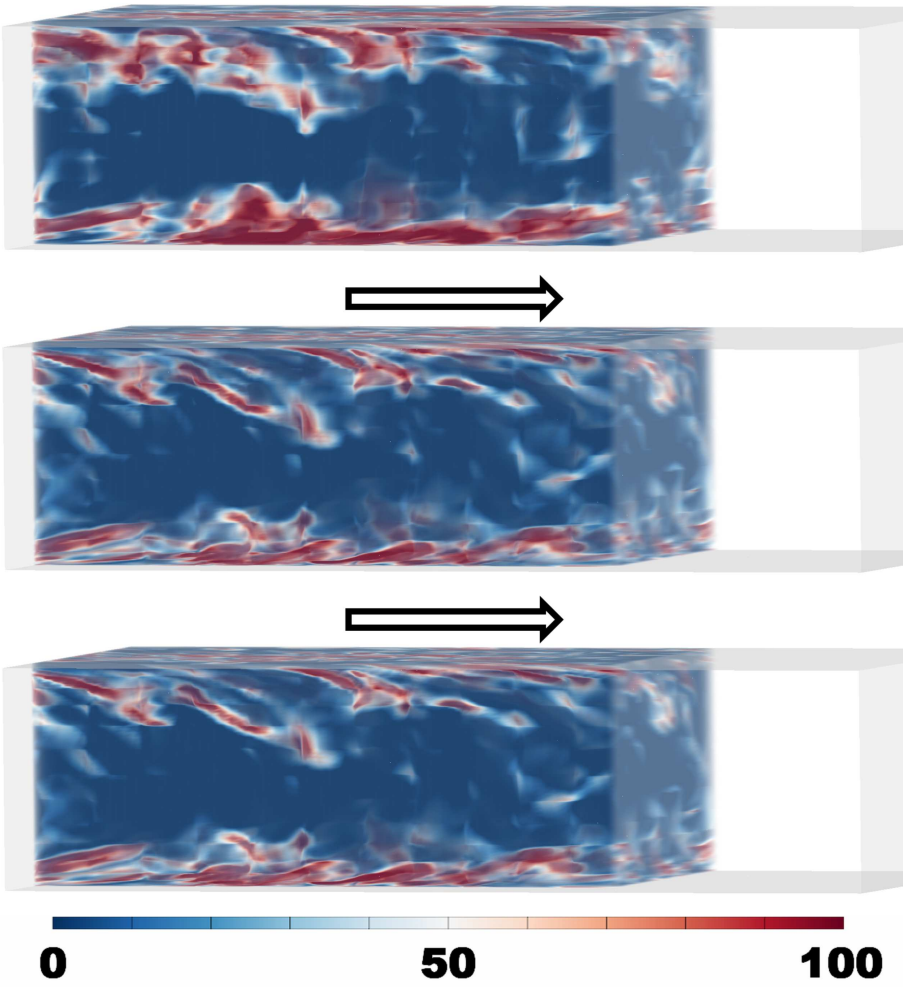

Figure 4.4: FTLE for the direct numerical simulation of a turbulent channel flow. The FTLE field visualized has been computed from the original field (top), the two (middle) and the four most dominant scales of motion (bottom). Observe that the focusing on the energetically most dominant scales of motion energy yields a more crispy and detailed output with finer lobes. Adding two more modes does not chance the output, even though just two modes where used for the first approximation. This indicates that the dissipative scales have to be interpreted as "noise" in the context of integration-based feature extraction. We refer to Paper C for further discussion.

Figure 4.5: Path lines in a exhaust manifold. All displayed path lines are seeded in the vicinity of the middle inlet pipe. The color encodes integration time (yellow to red). Particles moving away from the outlet (lower right corner) first are associated with back pressure.

study. All displayed path lines are seeded in the vicinity of the middle inlet pipe. The color encodes integration time (yellow to red). Particles moving away from the outlet (lower right corner) first are associated with back pressure.

In order to be able to compare results, we define analytically a set of "target path lines". Then we attempt to detect these path lines with both the path line attribute combinations proposed by Lež and the general path line attribute set proposed by us.

The comparison between our results and the previously published ones is based on the seeding position of the target path lines. We observe that the previous proposed path line attribute combinations systematically fail to detect path lines originating from the region highlighted in Fig. 4.6(a). Our method, on the other hand, shows a much better correspondence with the reference seed points, as Fig. 4.6(b) shows. The inset in both figures show the reference seeding points.

For further explanation of how exactly the analysis has been carried out, we refer to Sec. 4.2 in Paper D.

We infer that results based on the condensed path line attribute set proposed match, and to some extent even overgo, the reference results in previous published work.

(a) originally proposed method (b) our method

Figure 4.6: Analysis of an exhaust manifold. Comparison between the results achieved by using the attribute combinations used by Lež et al. [112] (a) the results achieved by the path line attribute set proposed in Paper D (b). The inset gives the reference seeding points we aim at detecting. We see that we are able to achieve better correspondence with the attributes proposed by us. A detailed description of the interactive visual flow analysis based on our path line attribute set is given in Sec. 4.2 in Paper D.

Chapter 5

Conclusions and Future Work

Understanding the governing principles for fluids in motion, especially turbulence, is still one of the grand challenges in physics and engineering [12]. A complete understanding of the underlying principles, also on an intuitive level[1], presents a canonic first step towards prediction and control of fluid flow phenomena of all types.

The phenomena we need to understand are both of local and global type, and often these two types of phenomena interact. The same phenomenon, on the other side, can usually be described in different manners[2], while each of the descriptions may have different strengths to capture a certain aspect of the semantical meaning of the phenomenon in question. Finally, other quantities that are not strictly related to the flow itself, may play an important role in more engineering type of applications.

With these considerations as a background, we identified the enrichment of classic flow visualization techniques by further semantic meaning, stemming from different aspects of the phenomena they originally describe, as a promising research topic.

Within the scope of the ph.d. work this thesis is the result of, we investigated ways to exploit physical and statistical tools to provide additional aspects of the semantics of phenomena in question. Furthermore we worked also on the enabling of incorporation of additional semantics by path line attributes. The latter opens for a broader application of interactive visual fluid analysis, especially in engineering.

In particular we provided a way to refine the semantic interpretation of the separation measure *finite-time Lyapunov exponents* (FTLE). FTLE has been a major research direction in the visualization of time-dependent flows over the last years, especially for the identification of Lagrangian coherent structures [157]. Understanding the exact semantic meaning of structures identified

[1] The governing equations have been known for a long time, but most of the intuition on fluid motion stems from experimentation and, recently, from direct numerical simulations [84].

[2] The Eulerian and Lagrangian reference frame being an example for different descriptor of the same phenomenon.

from FTLE fields is therefore of great importance for further research along these lines, and our research represents a step in that direction.

Our work on the flow field simplification and extraction on coherent features allows inherently for the identification of connections between local features extracted at a certain simplification level and their semantic meaning for the fluid in motion as a whole. This information can serve as a starting point for investigations about the mechanisms that drive the formation and destruction of the identified structures.

This first two research lines address chiefly the area of basic research in fluid mechanics as a user domain, and hence the immediate impact on the work of analysts dealing with more engineering-type of problems might be limited. To address the different requirement of the engineer-type of user, especially in the context of analysis based on path line attributes, we focused on the condensation of the attribute set which yields easier interaction with the data and gives the expert user more freedom to add descriptors that are of importance for the specific questions she or he wants to answer.

Possible lines of future work, resulting from the here presented work, are further investigation and systematic classification of different types of separation and their relation to classical separation measures, a more general framework to simultaneously treat Eulerian and Lagrangian representation of flow phenomena, especially for usage with path line attributes, and further incorporation of non-local flow properties in the extraction of coherent structures, e.g., enstrophy [137], to mention but a few.

Part II

Scientific Results

Bibliography

[1] D. K. Arrowsmith and C. M. Place. *An Introduction to Dynamical Systems*. Cambridge University Press, Cambridge, 1994.

[2] D. Asimov. Notes on the topology of vector fields and flows. Technical Report RNR-93-003, NASA Ames Research Center, 1993.

[3] D. Banks and B. Singer. A predictor-corrector technique for visualizing unsteady flow. *IEEE Transactions on Visualization and Computer Graphics*, 1(2):151–163, 1995.

[4] G. Berkooz. Observations on the proper orthogonal decomposition. In *Studies in Turbulence*, pages 229–247. Springer-Verlag, New York, 1992.

[5] G. Berkooz, P. Holmes, and J. L. Lumley. The proper orthogonal decomposition in the analysis of turbulent flows. *Annual Review of Fluid Mechanics*, 25:539–575, January 1993.

[6] S. L. Brunton and C. W. Rowley. Fast computation of finite-time lyapunov exponent fields for unsteady flows. *Chaos*, 20(1):1–12, 2010.

[7] R. Bürger, P. Muigg, H. Doleisch, and H. Hauser. Interactive cross-detector analysis of vortical flow data. In *Proceedings of the 5th International Conference on Coordinated & Multiple Views in Exploratory Visualization (CMV 2007)*, pages 98–110, 2007.

[8] R. Bürger, P. Muigg, H. Doleisch, and H. Hauser. Interactive cross-detector analysis of vortical flow data. In *Proceedings of CMV 2007*, pages 98–110. IEEE, 2007.

[9] R. Bürger, P. Muigg, M. Ilčík, H. Doleisch, and H. Hauser. Integrating local feature detectors in the interactive visual analysis of flow simulation data. In Museth, Möller, and Ynnerman, editors, *Data Visualization 2007: Proceedings of the 9th Joint* EUROGRAPHICS – IEEE VGTC *Symp. on Visualization (EuroVis 2007)*, pages 171–178. A K Peters, 2007.

[10] J. Carlson, A. Jaffe, and A. Wiles, editors. *The Millenium Prize Problems*. American Mathematical Society, 2006.

[11] R. B. Cattell. The scree test for the number of factors. *Multivariate Behavioral Research*, 1(2):245–276, 1966.

[12] A. Celani. The frontiers of computing in turbulence: challenges and

perspectives. *Journal of Turbulence*, 8(34):1–9, 2007.

[13] P. Chakraborty, S. Balanchandar, and R. J. Adrian. On the Relationships Between Local Vortex Identification Schemes. *Journal of Fluid Mechanics*, 535:189–214, 2005.

[14] M. Chong, A. Perry, and B. Cantwell. A general classification of three-dimensional flow fields. *Physics of Fluids A*, 2(5):765–777, 1990.

[15] A. B. Costello and J. W. Osborne. Best practices in exploratory factor analysis: Four recommendations for getting the most from your analysis. *Practical Assessment, Research & Evaluation*, 10:173–178, 2005.

[16] R. Cucitore, M. Quadrio, and A. Baron. On the effectiveness and limitations of local criteria for the identification of a vortex. *European Journal of Mechanics - B/Fluids*, 18(2):261 – 282, 1999.

[17] W. J. Davenport, C. M. Vogel, and J. S. Zsoldos. Flow structure produced by the interaction and merger of a pair of co-rotating wing-tip vortices. *Journal of Fluid Mechanics*, 394:357–377, 1999.

[18] P. A. Davidson and P. Davidson. *Turbulence: An Introduction for Scientists and Engineers*. Oxford University Press, July 2004.

[19] W. de Leeuw and R. van Liere. Collapsing Flow Topology Using Area Metrics. In *Proceedings of IEEE Visualization '99*, pages 349–354, 1999.

[20] W. de Leeuw and R. van Liere. Visualization of global flow structures using multiple levels of topology. In *Data Visualization '99: Proceedings of the 1st Joint* EUROGRAPHICS – IEEE TCVG *Symp. on Visualization (VisSym '99)*, pages 45–52. Springer, 1999.

[21] W. C. de Leeuw and R. van Liere. Collapsing flow topology using area metrics. In *Proc. of IEEE Visualization*, pages 349–354, Washington, DC, USA, 1999. IEEE Computer Society.

[22] S. Depardon, J. Lasserre, L. Brizzi, and J. Borée. Automated topology classification method for instantaneous velocity fields. *Experiments in Fluids*, 42(5):697–710, 2007.

[23] T. K. Dey, J. A. Levine, and R. Wenger. A Delaunay Simplification Algorithm for Vector Fields. In *Proceedings of the 15th Pacific Conference on Computer Graphics and Applications*, pages 281–290. IEEE Computer Society, 2007.

[24] H. Doleisch. SimVis: Interactive visual analysis of large and time-dependent 3D simulation data. In *Proceedings of the 2007 Winter Conference on Simulation (WSC 2007)*, pages 712–720, 2007.

[25] H. Doleisch, M. Gasser, and H. Hauser. Interactive feature specification

for focus+context visualization of complex simulation data. In Bonneau, Hahmann, and Hansen, editors, *Data Visualization 2003: Proceedings of the 5th Joint* EUROGRAPHICS – IEEE TCVG *Symp. on Visualization (VisSym 2003)*, pages 239–248. Eurographics, 2003.

[26] H. Doleisch and H. Hauser. Smooth brushing for focus+context visualization of simulation data in 3D. *Journal of WSCG*, 11(1-2):147–154, 2001.

[27] H. Doleisch and H. Hauser. Interactive visual exploration and analysis of multivariate simulation data. *Computing in Science Engineering*, 14(2):70–77, 2012.

[28] H. Doleisch, M. Mayer, M. Gasser, P. Priesching, and H. Hauser. Interactive feature specification for simulation data on time-varying grids. In *Proceedings of Conference Simulation & Visualization (SimVis 2005)*, pages 291–304, 2005.

[29] H. Doleisch, P. Muigg, and H. Hauser. Interactive visual analysis of hurricane isabel with SimVis. Technical Report TR-VRVis-2004-058, VRVis Research Center, Vienna, Austria, 2004.

[30] P. A. Durbin and B. A. Pettersson Reif. *Statistical Theory and Modeling for Turbulent Flows*. Wiley, 2nd edition, 2011.

[31] D. Eberly. *Ridges in Image and Data Analysis*. Computational Imaging and Vision. Kluwer Academic Publishers, 1996.

[32] D. Eberly, R. Gardner, B. Morse, S. Pizer, and C. Scharlach. Ridges for image analysis. *Journal of Mathematical Imaging and Vision*, 4(4):353–373, 1994.

[33] J. Ebling, A. Wiebel, C. Garth, and G. Scheuermann. Topology based flow analysis and superposition effects. In Hauser, Hagen, and Theisel, editors, *Topology-Based Methods in Visualization: Proceedings of the 1st TopoInVis Workshop (TopoInVis 2005)*, pages 91–103, 2007.

[34] G. Erlebacher, B. Jobard, and D. Weiskopf. Flow Textures: High-Resolution Flow Visualization. In C. D. Hansen and C. R. Johnson, editors, *The Visualization Handbook*, pages 279–293. Elsevier, Amsterdam, 2005.

[35] F. Ferstl, K. Bürger, H. Theisel, and R. Westermann. Interactive separating streak surfaces. *IEEE Transactions on Visualization and Computer Graphics*, 16(6):1569–1577, November - December 2010.

[36] P. Firby and C. Gardiner. *Surface Topology*, chapter 7, pages 115–135. Ellis Horwood Ltd., 1982.

[37] I. K. Fodor. A survey of dimension reduction techniques. Technical Report UCRL-ID-148494, Lawrence Livermore National Laboratory (LLNL), 2002.

[38] R. Fuchs and H. Hauser. Visualization of multi-variate scientific data. *Computer Graphics Forum*, 28(6):1670–1690, 2009.

[39] R. Fuchs, J. Kemmler, B. Schindler, J. Waser, F. Sadlo, H. Hauser, and R. Peikert. Toward a lagrangian vector field topology. *Computer Graphics Forum*, 29(3):1163–1172, june 2010.

[40] R. Fuchs, R. Peikert, H. Hauser, F. Sadlo, and P. Muigg. Parallel vectors criteria for unsteady flow vortices. *IEEE Transactions on Visualization and Computer Graphics*, 14(3):615–626, 2008.

[41] R. Fuchs, R. Peikert, F. Sadlo, B. Alsallakh, and M. E. Gröller. Delocalized Unsteady Vortex Region Detectors. In *Proceedings VMV 2008*, pages 81–90, 2008.

[42] C. Garth, F. Gerhardt, X. Tricoche, and H. Hagen. Efficient computation and visualization of coherent structures in fluid flow applications. *IEEE Transactions on Visualization and Computer Graphics*, 13(6):1464–1471, Sep 2007.

[43] C. Garth, G.-S. Li, X. Tricoche, C. D. Hansen, and H. Hagen. Visualization of coherent structures in transient 2d flows. In H.-C. Hege and G. S. K. Polthier, editors, *Topology-Based Methods in Visualization II*, pages 1–13, 2009.

[44] C. Garth, X. Tricoche, and G. Scheuermann. Tracking of vector field singularities in unstructured 3D time-dependent datasets. In *Proceedings of IEEE Visualization 2004*, pages 329–336, 2004.

[45] C. Garth, A. Wiebel, X. Tricoche, K. I. Joy, and G. Scheuermann. Lagrangian visualization of flow-embedded surface structures. *Computer Graphics Forum*, 27(3):1007–1014, 2008.

[46] P. E. Gill, W. Murray, and M. Wright. *Numerical Linear Algebra and Optimization*. Addison Wesley Publishing Company, 1st edition, 1991.

[47] J.-M. Ginoux and B. Rossetto. Differential Geometry and Mechanics: Applications to Chaotic Dynamical Systems. *International Journal of Bifurcation and Chaos*, 16(4):887–910, 2006.

[48] M. N. Glauser. *Coherent Structures in the Axisymmetric Turbulent Jet Mixing Layer*. Ph.D. dissertation, State University of New York at Buffalo, Buffalo, NY, 1987.

[49] A. Globus, C. Levit, and T. Lasinski. A tool for visualizing the topology of

three-dimensional vector fields. In *Proceedings of IEEE Visualization '91*, pages 33–40, 1991.

[50] I. Goldhirsch, P. L. Sulem, and S. A. Orszag. Stability and Lyapunov stability of dynamical systems: A differential approach and a numerical method. *Physica D*, 27(3):311–337, aug 1987.

[51] G. H. Golub and C. F. Van Loan. *Matrix Computations*. Johns Hopkins Studies in Mathematical Sciences. The Johns Hopkins University Press, 3rd edition, 1996.

[52] R. C. Gonzalez and R. E. Woods. *Digital Image Processing (3rd Edition)*. Prentice-Hall, Inc., 3rd edition, 2006.

[53] M. A. Green, C. W. Rowley, and G. Haller. Detection of lagrangian coherent structures in three-dimensional turbulence. *Journal of Fluid Mechanics*, 572:111–120, 2007.

[54] D. Gresh, B. Rogowitz, R. Winslow, D. Scollan, and C. Yung. WEAVE: a system for visually linking 3-d and statistical visualizations, applied to cardiac simulation and measurement data. In *Proceedings of IEEE Visualization 2000*, pages 489–492, 2000.

[55] E. Gröller, H. Löffelmann, and R. Wegenkittl. Visualization of dynamical systems. *Future Generation Computer Systems*, 15(1):75–86, 1999.

[56] J. Guckenheimer and P. Holmes. *Nonlinear Oscillations, Dynamical Systems and Bifurcations of Vector Fields*, volume 42 of *Applied Mathematical Sciences*. Springer, New York, Berlin, Heidelberg, Tokyo, 1983.

[57] E. Hairer, S. P. Nørsett, and G. Wanner. *Solving Ordinary Differential Equations I*. Springer Series in Computational Mathematics. Springer, 2nd edition, 1993.

[58] G. Haller. Finding finite-time invariant manifolds in two-dimensional velocity fields. *Chaos*, 10(1):99–108, 2000.

[59] G. Haller. Distinguished material surfaces and coherent structures in three-dimensional fluid flows. *Physica D*, 149:248–277, 2001.

[60] G. Haller. Lagrangian coherent structures from approximate velocity data. *Physics of Fluids*, 14:1851–1861, 2002.

[61] G. Haller. An objective definition of a vortex. *Journal of Fluid Mechanics*, 525:1–26, 2005.

[62] G. Haller. Variational theory of hyperbolic Lagrangian coherent structures. *Physica D*, 240:574–598, 2011.

[63] G. Haller and T. Sapsis. Lagrangian coherent structures and the smallest finite-time lyapunov exponent. *Chaos*, 21(2):023115, (submitted) 2011.

[64] R. Haralick. Ridges and valleys on digital images. *Computer Vision, Graphics, and Image Processing*, 22(1):28–38, 1983.

[65] H. H. Harman. *Modern Factor Analysis*. The University of Chicago Press, Chicago, IL U.S.A., 3rd edition, 1976.

[66] Hauser, Hagen, and Theisel. *Topology-Based Methods in Visualization: Proceedings of the 1st TopoInVis Workshop (TopoInVis 2005)*. Springer, 2007.

[67] H. Hauser. Generalizing focus+context visualization. In *Scientific Visualization: Proceedings of the respective Dagstuhl Seminar in 2003*, pages 305–327, 2003.

[68] H. Hauser, R. Laramee, and H. Doleisch. Topology-based versus feature-based flow analysis – challenges and an application. In Hauser, Hagen, and Theisel, editors, *Topology-Based Methods in Visualization: Proceedings of the 1st TopoInVis Workshop (TopoInVis 2005)*, pages 79–90. Springer, 2007.

[69] H. Hauser and M. Mlejnek. Interactive volume visualization of complex flow semantics. In *Proceedings of the 8th Fall Workshop on Vision, Modeling and Visualization (VMV 2003)*, pages 191–198, 2003.

[70] M. Hayes. On strain and straining. *Archive for Rational Mechanics and Analysis*, 100(3):265–273, September 1988.

[71] B. Heckel, G. Weber, B. Hamann, and K. Joy. Construction of vector field hierarchies. In *Proceedings of IEEE Visualization '99*, pages 19–26, 1999.

[72] H.-C. Hege, K. Polthier, and G. Scheuermann. *Topology-Based Methods in Visualization II*. Springer, 2008.

[73] J. Helman and L. Hesselink. Representation and display of vector field topology in fluid flow data sets. *Computer*, 22(8):27–36, 1989.

[74] J. Helman and L. Hesselink. Representation and display of vector field topology in fluid flow data sets. *IEEE Computer*, 22(8):27–36, 1989.

[75] J. Helman and L. Hesselink. Visualizing vector field topology in fluid flows. *IEEE Computer Graphics and Applications*, 11:36–46, 1991.

[76] S. Herzog. *The Large Scale Structure in the Near-Wall Region of Turbulent Pipe Flow*. Ph.D. dissertation, Cornell University, Ithaca, NY, 1986.

[77] L. Hesselink, J. Helman, and P. Ning. Quantitative image processing in fluid mechanics. *Experimental Thermal and Fluid Science*, 5(5):605 – 616, 1992. Special Issue on Experimental Methods in Thermal and Fluid

Science.

[78] M. Hlawatsch, F. Sadlo, and D. Weiskopf. Hierarchical line integration. *IEEE Transactions on Visualization and Computer Graphics*, 17(8):1148 – 1163, 2011.

[79] C.-C. Hsiung. *A first course in differential geometry*. Wiley, New York, 1981.

[80] J. C. R. Hunt, A. A. Wray, and P. Moin. Eddies, stream and convergence zones in turbulent flows. In *2. Proceedings of the 1988 Summer Program*, pages 193–208, 1988.

[81] J. Jeong and F. Hussain. On the identification of a vortex. *Journal of Fluid Mechanics*, 285:69–84, 1995.

[82] M. Jiang, R. Machiraju, and D. Thompson. Geometric verification of swirling features in flow fields. In *Proceedings of IEEE Visualization 2002*, pages 307–314, 2002.

[83] M. Jiang, R. Machiraju, and D. Thompson. Detection and visualization of vortices. In *The Visualization Handbook*, pages 295–309. Academic Press, 2005.

[84] J. Jiménez. Computing high-reynolds-number turbulence: will simulations ever replace experiments? *Journal of Turbulence*, 4(22):1–14, 2003.

[85] H. Jänicke, M. Böttinger, X. Tricoche, and G. Scheuermann. Automatic detection and visualization of distinctive structures in 3d unsteady multifields. *Computer Graphics Forum*, 27(3):767–774, 2008.

[86] H. Jänicke, A. Wiebel, G. Scheuermann, and W. Kollmann. Multifield visualization using local statistical complexity. *IEEE Transactions on Visualization and Computer Graphics*, 13(6):1384–1391, 2007.

[87] R. A. Johnson and D. W. Wichern. *Applied Multivariate Statistical Analysis*. Pearson Prentice Hall, Upper Saddle River, NJ U.S.A., 6. ed edition, 2007.

[88] D. W. Jordan and P. Smith. *Nonlinear ordinary differential equations : an introduction for scientists and engineers*. Oxford Applied and Engineering Mathematics. Oxford University Press, 4th ed. edition, 2007.

[89] H. F. Kaiser. The application of electronic computers to factor analysis. *Educational and Psychological Measurement*, 20(1):141–151, 1960.

[90] J. Kasten, I. Hotz, B. R. Noack, and H.-C. Hege. On the Extraction of Long-living Features in Unsteady Fluid Flows. In Pascucci, Tricoche, Hagen, and Tierny, editors, *Topological Data Analysis and Visualization: Theory, Algorithms and Applications (TopoInVis 2009)*, pages 115–127.

Springer, 2009.

[91] J. Kasten, C. Petz, I. Hotz, B. R. Noack, and H.-C. Hege. Localized finite-time lyapunov exponent for unsteady flow analysis. In M. A. Magnor, B. Rosenhahn, and H. Theisel, editors, *Proceedings of the Workshop on Vision, Modeling, and Visualization (VMV 2009)*, pages 265–276, 2009.

[92] J. Kasten, J. Reininghaus, I. Hotz, and H.-C. Hege. Two-dimensional time-dependent vortex regions based on the acceleration magnitude. *IEEE Transactions on Visualization and Computer Graphics*, 17(12):2080 –2087, 2011.

[93] J. Kehrer, F. Ladstädter, P. Muigg, H. Doleisch, A. Steiner, and H. Hauser. Hypothesis generation in climate research with interactive visual data exploration. *IEEE Transactions on Visualization and Computer Graphics (IEEE TVCG)*, 14(6):1579–1586, Oct 2008.

[94] D. Keim, F. Mansmann, J. Schneidewind, and H. Ziegler. Challenges in visual data analysis. *Proceedings of the 10th International Conference on Information Visualization (IV 2006)*, pages 9–16, 2006.

[95] C. T. Kelley. *Solving nonlinear equations with Newton's method*. Fundamentals of Algorithms. Society for Industrial and Applied Mathematics (SIAM), Philadelphia, PA, 2003.

[96] D. Kenwright. Automatic detection of open and closed separation and attachment lines. In *Proceedings of IEEE Visualization '98*, pages 151–158, 1998.

[97] D. Kenwright, C. Henze, and C. Levit. Feature extraction of separation and attachment lines. *IEEE Transactions on Visualization and Computer Graphics*, 5(2):135–144, 1999.

[98] J. J. Koenderink and A. van Doorn. Local features of smooth shape: Ridges and courses. *Proceedings of SPIE: Geometric Methods in Computer Vision II*, 2031:2–13, 1993.

[99] Z. Konyha, K. Matković, D. Gračanin, M. Jelović, and H. Hauser. Interactive visual analysis of families of function graphs. *IEEE Transactions on Visualization and Computer Graphics*, 12(6):1373–1385, 2006.

[100] R. Kosara, H. Doleisch, M. Gasser, and H. Hauser. The SimVis system for interactive visual analysis of flow simulation data. In *Proceedings of Conference Virtual Product Development (VPD) in Automotive Engineering (VDP 2004)*, 2004.

[101] J. Kostas, J. Soria, and M. S. Chong. A comparison between snapshot POD analysis of PIV velocity and vorticity data. *Experiments in Fluids*, 38:146–160, 2005.

[102] L. Kourentis and E. Konstantinidis. Uncovering large-scale coherent structures in natural and forced turbulent wakes by combining piv, pod, and ftle. *Experiments in Fluids*, 52:749–763, 2012.

[103] B. Krauskopf and H. M. Osinga. Two-dimensional global manifolds of vector fields. *Chaos*, 9(3):768–774, 1999.

[104] D. Laney, P.-T. Bremer, A. Mascarenhas, P. Miller, and V. Pascucci. Understanding the structure of the turbulent mixing layer in hydrodynamic instabilities. *Visualization and Computer Graphics, IEEE Transactions on*, 12(5):1053 –1060, Sept./Oct. 2006.

[105] R. Laramee, C. Garth, H. Doleisch, J. Schneider, H. Hauser, and H. Hagen. Visual analysis and exploration of fluid flow in a cooling jacket. In *Proceedings of IEEE Visualization 2005*, pages 623 – 630, 2005.

[106] R. Laramee, H. Hauser, H. Doleisch, B. Vrolijk, F. Post, and D. Weiskopf. The state of the art in flow visualization: Dense and texture-based techniques. *Computer Graphics Forum*, 23(2):143–161, 2004.

[107] R. Laramee, H. Hauser, L. Zhao, and F. Post. Topology-based flow visualization, the state of the art. In Hauser, Hagen, and Theisel, editors, *Topology-Based Methods in Visualization: Proceedings of the 1st TopoInVis Workshop (TopoInVis 2005)*, pages 1–20, 2007.

[108] Y. Lavin, R. Batra, and L. Hesselink. Feature comparisons of vector fields using earth mover's distance. In *Proceedings of IEEE Visualization '98*, pages 103–110, 1998.

[109] D. J. Lehmann and H. Theisel. Discontinuities in continuous scatterplots. *IEEE Transactions on Visualization and Computer Graphics*, 16(6):1291 –1300, November - December 2010.

[110] Y. Levy, D. Degani, and A. Seginer. Graphical visualization of vortical flows by means of helicity. *AIAA Journal*, 28(8):1347–1352, 1990.

[111] Y. Levy, D. Degani, and A. Seginer. Graphical visualization of vortical flows by means of helicity. *AIAA Journal*, 28(8):1347–1352, 1990.

[112] A. Lež, A. Zajic, K. Matković, A. Pobitzer, M. Mayer, and H. Hauser. Interactive exploration and analysis of pathlines in flow data. In *Proceedings of the International Conference in Central Europe on Computer Graphics, Visualization and Computer Vision (WSCG 2011)*, pages 17–24, 2011.

[113] W. Li, B. Vallet, N. Ray, and B. Levy. Representing higher-order singularities in vector fields on piecewise linear surfaces. *IEEE Transactions on Visualization and Computer Graphics*, 12(5):1315–1322, 2006.

[114] T. Lindeberg. Edge detection and ridge detection with automatic scale selection. *International Journal of Computer Vision*, 30(2):117–154, 1998.

[115] D. Lipinski and K. Mohseni. A ridge tracking algorithm and error estimate for efficient computation of lagrangian coherent structures. *Chaos*, 20(1):1–9, 2010.

[116] C.-H. Lo and H.-S. Don. Invariant representation and matching of space curves. *Journal of Intelligent and Robotic Systems*, 28:125–149, June 2000.

[117] S. Lodha, N. Faaland, and J. Renteria. Topology preserving top-down compression of 2d vector fields using bintree and triangular quadtrees. *IEEE Transactions on Visualization and Computer Graphics*, 9(4):433–442, 2003.

[118] S. Lodha, J. Renteria, and K. Roskin. Topology preserving compression of 2D vector fields. In *Proceedings of IEEE Visualization 2000*, pages 343–350, 2000.

[119] H. Löffelmann, H. Doleisch, and E. Gröller. Visualizing dynamical systems near critical points. In *Spring Conference on Computer Graphics and its Applications*, pages 175–184, Budmerice, Slovakia, 1998.

[120] H. Löffelmann and E. Gröller. Enhancing the visualization of characteristic structures in dynamical systems. In D. Bartz, editor, *Proceedings of the 9th* EUROGRAPHICS *Workshop on Visualization in Scientific Computing '98*, pages 59–68. Springer, 1998.

[121] H. Löffelmann, T. Kučera, and E. Gröller. Visualizing Poincaré maps together with the underlying flow. In H.-C. Hege and K. Polthier, editors, *Mathematical Visualization*, pages 315–328. Springer, 1998.

[122] H. J. Lugt. The dilemma of defining a vortex. In U. Mueller, K. G. Roesner, and B. Schmidt, editors, *Recent Developments in Theoretical and Experimental Fluid Mechanics: Compressible and Incompressible Flows*, pages 309–321. Springer, 1979.

[123] J. L. Lumley. The structure of inhomogeneous turbulent flows. In *Atmospheric Turbulence and Radio Wave Propagation*, pages 166–178. Elsevier, 1967.

[124] K. Mahrous, J. Bennett, B. Hamann, and K. Joy. Improving topological segmentation of three-dimensional vector fields. In Bonneau, Hahmann, and Hansen, editors, *Data Visualization 2003: Proceedings of the 5th Joint* EUROGRAPHICS – IEEE TCVG *Symp. on Visualization (VisSym 2003)*, pages 203–212. Eurographics, 2003.

[125] K. Mahrous, J. Bennett, G. Scheuermann, B. Hamann, and K. I. Joy.

Topological segmentation in three-dimensional vector fields. *IEEE Transactions on Visualization and Computer Graphics*, 10(2):198–205, 2004.

[126] S. Mann and A. Rockwood. Computing singularities of 3D vector fields with geometric algebra. In *Proceedings of IEEE Visualization 2002*, pages 283–289, 2002.

[127] A. Martin and M. Ward. High dimensional brushing for interactive exploration of multivariate data. In *Proceedings of IEEE Visualization '95*, pages 271–278, 1995.

[128] G. E. Mase. *Continuum Mechanics*. Schaum's Outline Series. McGraw-Hill, 1st edition, 1969.

[129] G. T. Mase. *Continuum Mechanics for Engineers*. CRC Press, 1999.

[130] K. Matković, D. Gračanin, M. Jelović, and H. Hauser. Interactive visual steering – rapid visual prototyping of a common rail injection system. *IEEE Transactions on Visualization and Computer Graphics*, 14(6):1699–1706, 2008.

[131] K. Matković, M. Jelović, J. Jurić, Z. Konyha, and D. Gračanin. Interactive visual analysis and exploration of injection systems simulations. In *Proceedings of IEEE Visualization 2005*, pages 50–57, 2005.

[132] R. McGill, J. W. Tukey, and W. A. Larsen. Variations of Box Plots. *The American Statistician*, 32(1):12–16, 1978.

[133] T. McLoughlin, R. S. Laramee, R. Peikert, F. H. Post, and M. Chen. Over Two Decades of Integration-Based, Geometric Flow Visualization. *Computer Graphics Forum*, 29(6):1807–1829, 2010.

[134] H. Miura and S. Kida. Identification of tubular vortices in turbulence. *Journal of the Physical Society of Japan*, 66:1331–1334, 1997.

[135] P. Muigg, J. Kehrer, S. Oeltze, H. Piringer, H. Doleisch, B. Preim, and H. Hauser. A four-level focus+context approach to interactive visual analysis of temporal features in large scientific data. *Computer Graphics Forum*, 27(3):775–782, 2008.

[136] H. Obermaier, M. Hering-Bertram, J. Kuhnert, and H. Hagen. Volume deformations in grid-less flow simulations. *Computer Graphics Forum*, 28(3):879–886, 2009.

[137] K. G. Oetzel and G. K. Vallis. Strain, vortices, and the enstrophy inertial range in two-dimensional turbulence. *Physics of Fluids*, 9:2991–3004, oct 1997.

[138] A. B. Olcay, T. S. Pottebaum, and P. S. Krueger. Sensitivity of lagrangian coherent structure identification to flow field resolution and random er-

rors. *Chaos*, 20(1):1–10, 2010.

[139] M. Otto, T. Germer, H.-C. Hege, and H. Theisel. Uncertain 2d vector field topology. *Computer Graphics Forum*, 29(2):347–356, 2010.

[140] M. Otto, T. Germer, and H. Theisel. Uncertain topology of 3d vector fields. In *Pacific Visualization Symposium (PacificVis), 2011 IEEE*, pages 67 –74, 2011.

[141] J. Palacios and E. Zhang. Rotational symmetry field design on surfaces. *ACM Transactions on Graphics*, 26(3):55, 2007.

[142] T. Peacock and J. Dabiri. Introduction to focus issue: Lagrangian coherent structures. *Chaos*, 20(1):1–3, 2010.

[143] K. Pearson. On lines and planes of closest fit to systems of points in space. *Philosophical Magazine*, 2(6):559–572, 1901.

[144] J. M. Pedersen. *Analysis of Planar Measurements of Turbulent Flows*. PhD thesis, Technical University of Denmark, February 2003.

[145] R. Peikert and M. Roth. The "parallel vectors" operator – a vector field visualization primitive. In *Proceedings of IEEE Visualization '99*, pages 263–270, 1999.

[146] R. Peikert and F. Sadlo. Topology-guided visualization of constrained vector fields. In Hauser, Hagen, and Theisel, editors, *Topology-Based Methods in Visualization: Proceedings of the 1st TopoInVis Workshop (TopoInVis 2005)*, pages 21–34, 2007.

[147] R. Peikert and F. Sadlo. Height Ridge Computation and Filtering for Visualization. In I. Fujishiro, H. Li, and K.-L. Ma, editors, *Proceedings of Pacific Vis 2008*, pages 119–126, 2008.

[148] R. Peikert and F. Sadlo. Flow topology beyond skeletons: Visualization of features in recirculating flow. In Hege, Polthier, and Scheuermann, editors, *Topology-Based Methods in Visualization II: Proceedings of the 2nd TopoInVis Workshop (TopoInVis 2007)*, pages 145–160, 2009.

[149] R. Peikert and F. Sadlo. Topologically Relevant Stream Surfaces for Flow Visualization. In H. Hauser, editor, *Proc. Spring Conference on Computer Graphics*, pages 43–50, 2009.

[150] A. Perry and M. Chong. A description of eddying motions and flow patterns using critical point concepts. *Annual Review of Fluid Mechanics*, 19:125–155, 1987.

[151] A. Perry and M. Chong. Topology of Flow Patterns in Vortex Motions and Turbulence. *Applied Scientific Research*, 53:357–374, 1994.

[152] A. E. Perry and D. K. M. Tan. Simple three-dimensional vortex motions

in coflowing jets and wakes. *Journal of Fluid Mechanics*, 141:197–231, 1984.

[153] F. Petronetto, A. Paiva, M. Lage, G. Tavares, H. Lopes, and T. Lewiner. Meshless helmholtz-hodge decomposition. *Transactions on Visualization and Computer Graphics*, 16(2):338–342, March 2010.

[154] C. Petz, J. Kasten, S. Prohaska, and H.-C. Hege. Hierarchical vortex regions in swirling flow. *Computer Graphics Forum*, 28(3):863–870, 2009.

[155] H. Piringer, W. Berger, and H. Hauser. Quantifying and comparing features in high-dimensional datasets. In *Proceedings of the 12th International Conference on Information Visualization (IV 2008)*, pages 240–245, 2008.

[156] A. Pobitzer, R. Peikert, R. Fuchs, B. Schindler, A. Kuhn, H. Theisel, K. Matković, and H. Hauser. On the way towards topology-based visualization of unsteady flow – the state of the art. In H. Hauser and E. Reinhard, editors, *Eurographics 2010 – State of the Art Reports*. Eurographics Association, May 2010.

[157] A. Pobitzer, R. Peikert, R. Fuchs, B. Schindler, A. Kuhn, H. Theisel, K. Matkovic, and H. Hauser. The state of the art in topology-based visualization of unsteady flow. *Computer Graphics Forum*, 30(6):1789–1811, 2011.

[158] A. Pobitzer, R. Peikert, R. Fuchs, H. Theisel, and H. Hauser. Filtering of FTLE for Visualizing Spatial Separation in Unsteady 3D Flow. In R. Peikert, H. Hauser, H. Carr, and R. Fuchs, editors, *Topological Methods in Data Analysis and Visualization II*, pages 237–253. Springer, 2012.

[159] H. Poincaré. *Les méthodes nouvelles de la mécanique céleste*. Gauthier-Villars, 1892.

[160] K. Polthier and E. Preuss. Identifying Vector Fields Singularities using a Discrete Hodge Decomposition. In H. C. Hege and K. Polthier, editors, *Visualization and Mathematics III*, pages 113–134. Springer Verlag, 2003.

[161] F. Post, B. Vrolijk, H. Hauser, R. Laramee, and H. Doleisch. Feature extraction and visualization of flow fields. In *Eurographics 2002 State-of-the-Art Reports*, pages 69–100, Saarbrücken Germany, 2002.

[162] F. Post, B. Vrolijk, H. Hauser, R. Laramee, and H. Doleisch. The state of the art in flow visualization: Feature extraction and tracking. *Computer Graphics Forum*, 22(4):775–792, 2003.

[163] F. Reinders, I. A. Sadarjoen, B. Vrolijk, and F. H. Post. Vortex tracking and visualisation in a flow past a tapered cylinder. *Computer Graphics*

Forum, 21(4):675–682, 2002.

[164] J. Reininghaus, C. Lowen, and I. Hotz. Fast combinatorial vector field topology. *Visualization and Computer Graphics, IEEE Transactions on*, PP(99):1, 2010.

[165] J. Roberts. State of the art: Coordinated & multiple views in exploratory visualization. In *Proceedings of the 5th International Conference on Coordinated & Multiple Views in Exploratory Visualization (CMV 2007)*, pages 61–71, 2007.

[166] M. Roth and R. Peikert. A higher-order method for finding vortex core lines. In *Proceedings of IEEE Visualization '98*, pages 143–150, 1998.

[167] I. Sadarjoen and F. Post. Geometric methods for vortex extraction. In Gröller, Löffelmann, and Ribarsky, editors, *Data Visualization '99: Proceedings of the 1st Joint* EUROGRAPHICS – IEEE TCVG *Symp. on Visualization (VisSym '99)*, pages 53–62. Springer, 1999.

[168] F. Sadlo and R. Peikert. Efficient Visualization of Lagrangian Coherent Structures by Filtered AMR Ridge Extraction. *IEEE Transactions on Visualization and Computer Graphics*, 13(6):1456–1463, 2007.

[169] F. Sadlo and R. Peikert. Time-Dependent Visualization of Lagrangian Coherent Structures by Grid Advection. In Pascucci, Tricoche, Hagen, and Tierny, editors, *Topological Data Analysis and Visualization: Theory, Algorithms and Applications (TopoInVis 2009)*, pages 151–165. Springer, 2009.

[170] F. Sadlo and R. Peikert. Visualizing lagrangian coherent structures: A comparison to vector field topology. In Hege, Polthier, and Scheuermann, editors, *Topology-Based Methods in Visualization II: Proceedings of the 2nd TopoInVis Workshop (TopoInVis 2007)*, pages 15–29, 2009.

[171] F. Sadlo and D. Weiskopf. Time-Dependent 2-D Vector Field Topology: An Approach Inspired by Lagrangian Coherent Structures. *Computer Graphics Forum*, 29(1):88–100, 2010.

[172] J. Sahner, T. Weinkauf, and H.-C. Hege. Galilean invariant extraction and iconic representation of vortex core lines. In Brodlie, Duke, and Joy, editors, *Data Visualization 2005: Proceedings of the 7th Joint* EUROGRAPHICS – IEEE VGTC *Symp. on Visualization (EuroVis 2005)*, pages 151–160. A K Peters, 2005.

[173] J. Sahner, T. Weinkauf, N. Teuber, and H.-C. Hege. Vortex and strain skeletons in eulerian and lagrangian frames. *IEEE Transactions on Visualization and Computer Graphics*, 13(5):980–990, Sep 2007.

[174] T. Salzbrunn, C. Garth, G. Scheuermann, and J. Meyer. Pathline predi-

cates and unsteady flow structures. *Visual Computer*, 24(12):1039–1051, 2008.

[175] T. Salzbrunn, H. Jänicke, T. Wischgoll, and G. Scheuermann. The state of the art in flow visualization: partition-based techniques. In H. Hauser, S. Strassburger, and H. Theisel, editors, *Proc. of Simulation and Visualization 2008*, pages 75–92, 2008.

[176] T. Salzbrunn, H. Jänicke, T. Wischgoll, and G. Scheuermann. The state of the art in flow visualization: Partition-based techniques. In H. Hauser, S. Straßburger, and H. Theisel, editors, *SimVis*, pages 75–92. SCS Publishing House e.V., 2008.

[177] T. Salzbrunn and G. Scheuermann. Streamline predicates. *IEEE Transactions on Visualization and Computer Graphics*, 12(6):1601–1612, 2006.

[178] T. Salzbrunn and G. Scheuermann. Streamline predicates as flow topology generalization. In Hauser, Hagen, and Theisel, editors, *Topology-Based Methods in Visualization: Proceedings of the 1st TopoInVis Workshop (TopoInVis 2005)*, pages 65–77, 2007.

[179] G. Scheuermann, H. Hagen, H. Krüger, M. Menzel, and A. Rockwood. Visualization of higher order singularities in vector fields. In *Proceedings of IEEE Visualization '97*, pages 67–74, 1997.

[180] G. Scheuermann, B. Hamann, K. Joy, and W. Kollman. Visualizing local vector field topology. *SPIE Journal of Electronic Imaging*, 9(4):356–367, 2000.

[181] G. Scheuermann, H. Krüger, M. Menzel, and A. Rockwood. Visualizing non-linear vector field topology. *IEEE Transactions on Visualization and Computer Graphics*, 4(2):109–116, 1998.

[182] G. Scheuermann and X. Tricoche. Topological methods for flow visualization. In C. D. Hansen and C. R. Johnson, editors, *The Visualization Handbook*, pages 341–356. Elsevier, 2005.

[183] J. Seo and B. Shneiderman. A rank-by-feature framework for unsupervised multidimensional data exploration using low dimensional projections. In *Proc. of the IEEE InfoVis*, pages 65–72, Washington, DC, USA, 2004. IEEE Computer Society.

[184] S. Shadden, F. Lekien, and J. Marsden. Definition and properties of Lagrangian coherent structures from finite-time Lyapunov exponents in two-dimensional aperiodic flows. *Physica D Nonlinear Phenomena*, 212:271–304, Dec. 2005.

[185] S. C. Shadden, J. O. Dabiri, and J. E. Marsden. Lagrangian analysis of fluid transport in empirical vortex ring flows. *Physics of Fluids*,

18(4):047105, 2006.

[186] K. Shi, H. Theisel, H. Hauser, T. Weinkauf, K. Matković, H.-C. Hege, and H.-P. Seidel. Path line attributes – an information visualization approach to analyzing the dynamic behavior of 3d time-dependent flow fields. In Hege, Polthier, and Scheuermann, editors, *Topology-Based Methods in Visualization II: Proceedings of the 2nd TopoInVis Workshop (TopoInVis 2007)*, pages 75–88, 2009.

[187] K. Shi, H. Theisel, T. Weinkauf, H.-C. Hege, and H.-P. Seidel. Visualizing Transport Structures of Time-Dependent Flow Fields. *Computer Graphics and Applications*, 28(5):24–36, 2008.

[188] B. Shneiderman. The eyes have it: A task by data type taxonomy for information visualizations. In *Proc. of the 1996 IEEE Symp. on Visual Languages*, pages 336–343, 1996.

[189] L. Sirovich. Turbulence and the dynamics of coherent structures. *Quarterly of Applied Mathematics*, 45(3):561–590, September 1987.

[190] C. Spearman. Demonstration of formulæ for true measurement of correlation. *The Am. J. of Psychology*, 18(2):161–169, 1907.

[191] R. Strawn, D. Kenwriht, and J. Ahmad. Computer visualization of vortex wake systems. In *American Helicopter Society 54th Annual Forum*, 1998.

[192] D. D. Suhr. Principal component analysis vs. exploratory factor analysis. In *Proceedings of the Thirtieth Annual SAS® Users Group International Conference*. SAS Institute Inc., 2005.

[193] D. Sujudi and R. Haimes. Identification of swirling flow in 3d vector fields. Technical Report 95-1715, AIAA, 1995.

[194] W. Tang, P. W. Chan, and G. Haller. Accurate extraction of lagrangian coherent structures over finite domains with application to flight data analysis over hong kong international airport. *Chaos*, 20(1):1–8, 2010.

[195] A. Telea and J. van Wijk. Simplified representation of vector fields. In *Proceedings of IEEE Visualization '99*, pages 35–42, 1999.

[196] H. Theisel. *Vector Field Curvature and Applications*. PhD thesis, University of Rostock, November 1995.

[197] H. Theisel. Designing 2D vector fields of arbitrary topology. *Computer Graphics Forum*, 21(3):595–604, 2002.

[198] H. Theisel, C. Rössl, and H.-P. Seidel. Combining topological simplification and topology preserving compression for 2d vector fields. In *Proc. 11th Pacific Conference on Computer Graphics and Applications*, pages 419–423, 2003.

[199] H. Theisel, C. Rössl, and H.-P. Seidel. Compression of 2D vector fields under guaranteed topology preservation. *Computer Graphics Forum*, 22(3):333–342, 2003.

[200] H. Theisel, C. Rössl, and H.-P. Seidel. Using Feature Flow Fields for Topological Comparison of Vector Fields. In T. Ertl, B. Girod, G. Greiner, H. Niemann, H.-P. Seidel, E. Steinbach, and R. Westermann, editors, *PProceedings of the Workshop on Vision, Modeling, and Visualization (VMV 2003)*, pages 521–528. Akademische Verlagsgesellschaft Aka, November 2003.

[201] H. Theisel, C. Rössl, and T. Weinkauf. Topological representations of vector fields. In L. de Floriani and M. Spagnuolo, editors, *Shape Analysis and Structuring*, Mathematics and Visualization: Shape Analysis and Structuring, pages 215–240. Springer, Berlin, 2007.

[202] H. Theisel, J. Sahner, T. Weinkauf, H.-C. Hege, and H.-P. Seidel. Extraction of parallel vector surfaces in 3D time-dependent fields and application to vortex core line tracking. In *Proceedings of IEEE Visualization 2005*, pages 631–638, 2005.

[203] H. Theisel and H.-P. Seidel. Feature flow fields. In Bonneau, Hahmann, and Hansen, editors, *Data Visualization 2003: Proceedings of the 5th Joint* EUROGRAPHICS – IEEE TCVG *Symp. on Visualization (VisSym 2003)*, pages 141–148. Eurographics, 2003.

[204] H. Theisel and T. Weinkauf. Vector field metrics based on distance measures of first order critical points. *Journal of WSCG*, 10(3):121–128, 2002.

[205] H. Theisel, T. Weinkauf, H.-C. Hege, and H.-P. Seidel. Saddle connectors – an approach to visualizing the topological skeleton of complex 3d vector fields. In *Proceedings of IEEE Visualization 2003*, pages 225–232, 2003.

[206] H. Theisel, T. Weinkauf, H.-C. Hege, and H.-P. Seidel. Stream line and path line oriented topology for 2D time-dependent vector fields. In *Proceedings of IEEE Visualization 2004*, pages 321–328, 2004.

[207] H. Theisel, T. Weinkauf, H.-C. Hege, and H.-P. Seidel. Topological methods for 2D time-dependent vector fields based on stream lines and path lines. *IEEE Transactions on Visualization and Computer Graphics*, 11(4):383–394, 2005.

[208] H. Theisel, T. Weinkauf, H.-C. Hege, and H.-P. Seidel. Topological methods for 2d time-dependent vector fields based on stream lines and path lines. *IEEE TVCG*, 11(4):383–394, 2005.

[209] Y. Tong, S. Lombeyda, A. N. Hirani, and M. Desbrun. Discrete multiscale vector field decomposition. *ACM Transactions on Graphics*, 22(3):445–452, July 2003.

[210] X. Tricoche, G. Scheuermann, and H. Hagen. Continuous topology simplification of planar vector fields. In *Proceedings of IEEE Visualization 2001*, pages 159–166, 2001.

[211] X. Tricoche, G. Scheuermann, and H. Hagen. Topology-based visualization of time-dependent 2D vector fields. In Ebert, Favre, and Peikert, editors, *Data Visualization 2001: Proceedings of the 3rd Joint* EUROGRAPHICS – IEEE TCVG *Symp. on Visualization (VisSym 2001)*, pages 117–126. Springer, 2001.

[212] X. Tricoche, T. Wischgoll, G. Scheuermann, and H. Hagen. Topology tracking for the visualization of time-dependent two-dimensional flows. *Computers & Graphics*, 26(2):249–257, 2002.

[213] I. Trotts, D. Kenwright, and R. Haimes. Critical points at infinity: a missing link in vector field topology. In *Proc. NSF/DoE Lake Tahoe Workshop on Hierarchical Approximation and Geometrical Methods for Scientific Visualization*, 2000.

[214] c. Turkay, P. Filzmoser, and H. Hauser. Brushing dimensions – a dual visual analysis model for high-dimensional data. *IEEE Transactions on Visualization and Computer Graphics*, 17(12):2591–2599, 2011.

[215] M. Tutkun, P. B. V. Johansson, and W. K. George. Three-component vectorial proper orthogonal decomposition of axisymmetric wake behind a disk. *AIAA Journal*, 46:1118–1134, 2008.

[216] C. M. Velte, M. Tutkun, and W. K. George. New correction for random noise in spectra. *Experiments in Fluids*, (conditionally accepted), 2010.

[217] A. Vincent and M. Meneguzzi. The spatial structure and statistical properties of homogeneous turbulence. *Journal of Fluid Mechanics*, 225:1–20, Apr. 1991.

[218] C. E. Wasberg. Post-processing of marginally resolved spectral element data. In J. S. Hesthaven and E. M. Rønquist, editors, *Spectral and High Order Methods for Partial Differential Equations*, volume 76 of *Lecture Notes in Computational Science and Engineering*, pages 503–510. Springer Berlin Heidelberg, 2011.

[219] C. E. Wasberg, T. Gjesdal, B. A. Pettersson Reif, and Ø. Andreassen. Variational multiscale turbulence modelling in a high order spectral element method. *Journal of Computational Physics*, 228(19):7333–7356, 2009.

[220] T. Weinkauf and D. Günther. Separatrix persistence: Extraction of salient edges on surfaces using topological methods. *Computer Graphics Forum*, 28(5):1519–1528, July 2009.

[221] T. Weinkauf, J. Sahner, and H. Theisel. Cores of swirling particle motion in unsteady flows. *IEEE Transactions on Visualization and Computer Graphics*, 13(6):1759–1766, 2007.

[222] T. Weinkauf and H. Theisel. Curvature measures of 3D vector fields and their applications. *Journal of WSCG*, 10(2):507–514, 2002.

[223] T. Weinkauf and H. Theisel. Streak lines as tangent curves of a derived vector field. *IEEE Transactions on Visualization and Computer Graphics*, 16(6):1569 –1577, November - December 2010.

[224] T. Weinkauf, H. Theisel, A. V. Gelder, and A. Pang. Stable feature flow fields. *IEEE Transactions on Visualization and Computer Graphics*, 17(6):770–780, 2011.

[225] T. Weinkauf, H. Theisel, H.-C. Hege, and H.-P. Seidel. Topological construction and visualization of higher order 3D vector fields. *Computer Graphics Forum*, 23(3):469–478, 2004.

[226] T. Weinkauf, H. Theisel, K. Shi, H.-C. Hege, and H.-P. Seidel. Extracting higher order critical points and topological simplification of 3D vector fields. In *Proc. IEEE Visualization 2005*, pages 559–566, 2005.

[227] A. Wiebel, R. Chan, C. Wolf, A. Robitzki, A. Stevens, and G. Scheuermann. Topological Flow Structures in a Mathematical Model for Rotation-Mediated Cell Aggregation. In Pascucci, Tricoche, Hagen, and Tierny, editors, *Topological Data Analysis and Visualization: Theory, Algorithms and Applications (TopoInVis 2009)*, pages 193–204. Springer, 2009.

[228] A. Wiebel, C. Garth, and G. Scheuermann. Computation of localized flow for steady and unsteady vector fields and its applications. *IEEE Transactions on Visualization and Computer Graphics*, 13(4):641–651, July 2007.

[229] A. Wiebel, X. Tricoche, and G. Scheuermann. Topology based flow analysis and superposition effects. In H.-C. Hege and G. S. K. Polthier, editors, *Topology-Based Methods in Visualization II*, pages 31–43, 2009.

[230] T. Wischgoll and G. Scheuermann. Detection and visualization of closed streamlines in planar flows. *IEEE Transactions on Visualization and Computer Graphics*, 7(2):165–172, 2001.

[231] T. Wischgoll and G. Scheuermann. Locating closed streamlines in 3d vector fields. In Ebert, Brunet, and Navazo, editors, *Data Visualiza-*

tion 2002: Proceedings of the 4th Joint EUROGRAPHICS – IEEE TCVG *Symp. on Visualization (VisSym 2002)*, pages 227–232. Eurographics, 2002.

[232] T. Wischgoll, G. Scheuermann, and H. Hagen. Tracking closed streamlines in time dependent planar flows. In *Proceedings of the 6th Fall Workshop on Vision, Modeling and Visualization (VMV 2001)*, pages 447–454, 2001.

[233] J. Yang, M. O. Ward, E. A. Rundensteiner, and S. Huang. Visual hierarchical dimension reduction for exploration of high dimensional datasets. In *Proc. of VISSYM '03*, pages 19–28. Eurographics Association, 2003.

[234] S. Yoden and M. Nomura. Finite-time lyapunov stability analysis and its application to atmospheric dynamics. *Journal of the Atmospheric Sciences*, 50(11):1531–1543, 1993.

[235] E. Zhang, J. Hays, and G. Turk. Interactive tensor field design and visualization on surfaces. *IEEE Transactions on Visualization and Computer Graphics*, 13(1):94–107, 2007.

[236] X. Zheng and A. Pang. Topological lines in 3D tensor fields. In *Proceedings of IEEE Visualization 2004*, pages 313–320, 2004.

[237] X. Zheng, B. Parlett, and A. Pang. Topological lines in 3d tensor fields and discriminant hessian factorization. *IEEE Transactions on Visualization and Computer Graphics*, 11(4):395–407, 2005.

[238] H. Zou, T. Hastie, and R. Tibshirani. Sparse principal component analysis. *Journal of Computational and Graphical Statistics*, 15(2):265–286, jun. 2006.